Mon. Not. R. Astron. Soc. **394,** 1131–1147 (2009) doi:10.1111/j.1365-2966.2009.14414.x

The correlation of star formation quenching with internal galaxy properties and environment

Taysun Kimm,[1] Rachel S. Somerville,[2,3] Sukyoung K. Yi,[1⋆] Frank C. van den Bosch,[3] Samir Salim,[4] Fabio Fontanot,[3] Pierluigi Monaco,[5,6] Houjun Mo,[7] Anna Pasquali,[3] R. M. Rich[8] and Xiaohu Yang[9]

[1]*Department of Astronomy, Yonsei University, Seoul 120-749, Korea*
[2]*Space Telescope Science Institute, 3700 San Martin Dr, Baltimore, MD 21218, USA*
[3]*Max-Planck-Institut für Astronomie, Königstuhl 17, Heidelberg D-69117, Germany*
[4]*National Optical Astronomy Observatory, 950 North Cherry Ave., Tucson AZ 85719, USA*
[5]*Dipartimento di Astronomia, Università di Trieste, via Tiepolo 11, I-34143 Trieste, Italy*
[6]*INAF–Osservatorio Astronomico, Via Tiepolo 11, I-34143 Trieste, Italy*
[7]*Department of Astronomy, University of Massachusetts, Amherst, MA 01003-9305, USA*
[8]*Department of Physics and Astronomy, University of California, Los Angeles, CA 90095, USA*
[9]*Shanghai Astronomical Observatory, the Partner Group of MPA, Nandan Road 80, Shanghai 200030, China*

Accepted 2008 December 5. Received 2008 December 3; in original form 2008 October 1

ABSTRACT

We investigate the correlation of star formation quenching with internal galaxy properties and large-scale environment (halo mass) in empirical data and theoretical models. We make use of the halo-based group catalogue of Yang and collaborators, which is based on the Sloan Digital Sky Survey. Data from the Galaxy evolution explorer are also used to extract the recent star formation rate. In order to investigate the environmental effects, we examine the properties of 'central' and 'satellite' galaxies separately. For central galaxies, we are unable to conclude whether star formation quenching is primarily connected with halo mass or stellar mass, because these two quantities are themselves strongly correlated. For satellite galaxies, a nearly equally strong dependence on halo mass and stellar mass is seen. We make the same comparison for five different semi-analytic models based on three independently developed codes. We find that the models with active galactic nuclei feedback reproduce reasonably well the dependence of the fraction of central red and passive galaxies on halo mass and stellar mass. However, for satellite galaxies, the same models badly overproduce the fraction of red/passive galaxies and do not reproduce the empirical trends with stellar mass or halo mass. This *satellite overquenching problem* is caused by the too-rapid stripping of the satellites' hot gas haloes, which leads to rapid strangulation of star formation.

Key words: galaxies: clusters: general – galaxies: evolution – galaxies: formation – galaxies: ISM.

1 INTRODUCTION

Galaxies may be broadly divided into two categories: those that are forming stars fairly rapidly relative to their past averaged star formation rate (SFR) and those that show little recent star formation relative to their past average. It is well known that, at least at low redshift ($z \lesssim 1$), the former type tends to have blue colours and to be morphologically disc dominated, while the latter tends to have red colours and to be morphologically early type or spheroid dominated. Galaxies exhibit colour bimodalities throughout a wide range of cosmic history (Strateva et al. 2001; Baldry et al. 2004; Balogh et al. 2004; Bell et al. 2004; Blanton et al. 2005b). One of the fundamental questions in galaxy formation is: what are the main physical forces that regulate and in some cases quench star formation? Are these processes more closely correlated with *internal galaxy properties* such as mass or luminosity or *large-scale environment* (sometimes referred to as 'Nature or Nurture')?

There have been many studies on the impact of environment on galaxy properties. For example, Davis & Geller (1976) and many others found that early-type galaxies are more strongly clustered than the late types, and Dressler (1980) systematically demonstrated that the fraction of elliptical and S0 galaxies is higher in denser environments. Similarly, it is well known that galaxies in dense environments tend to be red and have depressed SFRs (Hashimoto et al. 1998; Lewis et al. 2002; Gomez et al. 2003; Balogh et al. 2004;

⋆E-mail: yi@yonsei.ac.kr

Kauffmann et al. 2004; Tanaka et al. 2004; Christlein & Zabludoff 2005; Poggianti et al. 2006). There are several physical processes associated with environment that may play a role in galaxy transformation. Major (near equal mass) mergers can transform spiral galaxies into ellipticals (Toomre & Toomre 1972; cf. Barnes 2002), and may also quench future star formation by ejecting the interstellar medium (ISM) from the galaxy via starburst, active galactic nuclei (AGN) or shock-driven winds (Cox et al. 2004; Murray, Quataert & Thompson 2005; Springel, Di Matteo & Hernquist 2005). In rich clusters, where the probability of merging is suppressed because of the large relative velocities of galaxies, galaxy 'harassment' (rapid encounters or fly-bys) may cause a less dramatic form of transformation by heating discs, perhaps causing the formation of a bar and growth of a spheroidal component (Moore, Lake & Katz 1998). Also, cold gas can be stripped out of the galaxy by tidal forces due to the background dark matter dominated potential of the cluster as well as ram pressure stripping by the intracluster medium (Gunn & Gott 1972; Abadi, Moore & Bower 1999; Quilis, Moore & Bower 2000; Chung et al. 2007). Similarly, the hot halo that provides future fuel for cooling and star formation may be efficiently stripped in dense environments, thus quenching further star formation by 'starvation' or 'strangulation' (Larson, Tinsley & Caldwell 1980; Balogh & Morris 2000; Bekki, Couch & Shioya 2002).

However, studies by van den Bosch et al. (2008a) and Tanaka et al. (2004) suggest that processes specific to clusters (e.g. ram pressure stripping) are not the main mechanisms for quenching star formation activity. Similar results were also found at higher redshift (e.g. Cooper et al. 2006). Moreover, both the morphological and spectrophotometric characteristics of galaxies are also known to be strongly correlated with their internal properties, such as luminosity, mass and internal velocity (Roberts & Haynes 1994; Kauffmann et al. 2003). More massive or luminous galaxies are more likely to be spheroid dominated, red and to have old stellar populations and little recent star formation. Indeed, Kauffmann et al. (2003) showed that galaxies appear to make a transition in all of these properties above a critical stellar mass of $\sim 3 \times 10^{10}\,\mathrm{M}_{\odot}$.

Again, there are various physical processes that one might expect to imprint this kind of dependence on internal properties. Supernova feedback has long been invoked as a mechanism that could heat and drive gas out of galaxies (Larson 1974; Dekel & Silk 1986), and is expected to be more effective in low-mass galaxies. There is also mounting observational evidence that AGN are associated with the quenching of star formation (Schawinski et al. 2006; Salim et al. 2007, hereafter S07; Schawinski et al. 2007b). AGN feedback is expected to have more impact on massive galaxies, which host larger mass black holes (e.g. Silk & Rees 1998).

The emerging picture is that AGN seem to have two modes of fuelling and also to couple to their surroundings in different ways. 'Bright-mode' AGN are associated with high (near Eddington) fuelling rates, and observationally with classical X-ray or optically bright quasars. The radiation emitted by these objects can couple with the cold gas in the galaxy, perhaps driving powerful winds that can drive the gas out of the galaxy and quench star formation (Di Matteo et al. 2005; Monaco & Fontanot 2005; Murray et al. 2005).

In contrast, many massive galaxies seem to contain AGN which are accreting at a small fraction of their Eddington rate, and which typically do not show classical quasar-like signatures such as bright X-ray radiation or broad emission lines. However, these objects are associated with the efficient production of radio jets, which may be able to couple with and heat the hot gas in the galaxy's halo (e.g. McNamara & Nulsen 2007). These objects are often referred to as 'radio-mode' AGN (Croton et al. 2006). This process is expected to be a function of both internal properties and environment: the bigger the black hole, the more energy can be tapped (and black hole mass is, of course, correlated with galaxy mass), and empirically it is known that the fraction of radio-detected galaxies increases strongly with stellar mass (Best et al. 2005) and halo mass (Pasquali et al. 2008). But as well, the radio jets must have a 'working surface' and therefore can only be effective in environments that can support a quasi-hydrostatic hot gas halo, such as groups and clusters. Galaxies in smaller mass haloes ($M_{\mathrm{halo}} \lesssim 10^{12}\,\mathrm{M}_{\odot}$) likely accrete most of their gas in a 'cold flow', and never form a hot halo (Birnboim & Dekel 2003; Kereš et al. 2005; Dekel & Birnboim 2006).

A great deal of recent progress has been made towards developing a comprehensive theory of galaxy formation. The semi-analytic approach, although it has its limitations, is a powerful and flexible tool for exploring detailed predictions based on this theory (e.g. White & Frenk 1991; Kauffmann, White & Guiderdoni 1993; Kauffmann et al. 1999; Somerville & Primack 1999; Cole et al. 2000; Somerville, Primack & Faber 2001; Springel et al. 2001; Benson et al. 2003; Hatton et al. 2003; Khochfar & Burkert 2003; Kang et al. 2005; Khochfar & Burkert 2005). Several groups have now implemented one or both modes of black hole growth and AGN feedback into their semi-analytic models (e.g. Bower et al. 2006; Croton et al. 2006; Monaco, Fontanot & Taffoni 2007; Somerville et al. 2008b, hereafter S08). There seems to be consensus that including these new processes leads to greatly improved agreement with key observations such as galaxy luminosity or mass functions and the galaxy colour–magnitude (CM) distribution or stellar mass versus specific star formation distribution. However, this necessitates including several new recipes and parameters associated with the poorly understood physics of black hole growth and AGN feedback. Each model contains somewhat different parametrizations and treatments of these processes, yet they all produce similar results for global quantities such as the galaxy luminosity function and CM distribution, no doubt in part because these observations were 'targets' that the modellers were trying to reproduce. One goal of our work here is to determine whether breaking down the fraction of quenched galaxies in the dual space of internal galaxy properties and environment can discriminate between these different treatments of AGN feedback.

The large and homogeneous data bases provided by modern surveys, such as Sloan Digital Sky Survey (SDSS) and Galaxy Evolution Explorer (GALEX), finally allow a statistically significant investigation of different subpopulations of galaxies. However, an obvious question that arises in any study of galaxy environment is exactly how to measure and characterize environment in observational samples. Clearly, it is desirable to span as broad a range of environments as possible, from isolated field galaxies to groups to rich clusters. The majority of the studies in the literature have parametrized environment in terms of the number of galaxies, either within a fixed metric aperture or by the distance of the nth nearest galaxy, where n is typically in the range 3–10. Although these indicators are straightforward to measure, they are not straightforward to interpret in physical terms or to compare with theoretical models (see discussions in Kauffmann et al. 2004 and Weinmann et al. 2006a, hereafter W06a). An alternate approach is to use a galaxy group catalogue, in which galaxies in an observational catalogue are not only grouped together into putatively gravitationally bound structures, but also the total mass of their associated dark matter halo (DMH) is estimated (Yang et al. 2007, hereafter Y07). Thus, the relationship between galaxy properties and DMH properties can be studied directly. Another advantage of this method is that galaxies can be separated into 'central' and 'satellite' populations.

Most of the environment-related transformation mechanisms described above (such as stripping) are expected to work only on satellite galaxies, so this offers a way to separate out the effects of different physical processes.

Here, we make use of a large galaxy group catalogue constructed from the SDSS using the halo-based galaxy group finder developed by Yang et al. (2005). These catalogues have already been used for several studies regarding the environment dependence of galaxy properties. W06a, using the version based on the SDSS Data Release 2, studied the correlations between colours, specific star formation rate (SSFR) and halo mass. Splitting the galaxy population into early and late types, based on their colours and SSFRs, they found that, at a fixed luminosity, the late- (early-) type fraction of galaxies increases (decreases) with decreasing halo mass. Using the much larger galaxy group catalogue of Y07, based on the SDSS Data Release (DR4), van den Bosch et al. (2008a) showed that, on average, satellite galaxies are redder and more concentrated than central galaxies of the same stellar mass. They also found that the colour and concentration differences of central–satellite pairs matched in stellar mass are completely independent of the mass of the host halo of the satellite galaxy. This indicates that satellite-specific transformation mechanisms are equally efficient in host haloes of all masses and rules against satellite transformation mechanisms that are thought to operate only in very massive haloes. Further support for this was provided by van den Bosch et al. (2008b) and Pasquali et al. (2008), who showed that, at fixed stellar mass, the average colours and concentrations, as well as the occurrence of star formation and AGN activity, reveal only a very weak dependence on halo mass (but see Weinmann et al. 2008).

Weinmann et al. (2006b) compared the fractions of red and blue galaxies in the SDSS group catalogue of W06a with the semi-analytic model of galaxy formation of Croton et al. (2006). Although this model accurately fits the global statistics of the galaxy population, the model predicts a red fraction of satellites that is much higher than observed (see also Baldry et al. 2006; Coil et al. 2008).

In this paper, we extend the study of Weinmann et al. (2006b) using the much larger galaxy group catalogue of Y07 and a larger suite of semi-analytic models. Another new aspect of our work here is that we augment the SDSS-based galaxy properties in the group catalogue with information derived from the GALEX–SDSS matched sample of S07. The S07 analysis provides complementary quantities such as stellar masses and SFRs based on the two GALEX UV bands plus five-band SDSS photometry. The UV provides a much more sensitive probe of the recent star formation history of a galaxy than optical colours alone, which reflect the highly degenerate effects of stellar populations, metallicity and dust extinction (Yi et al. 2005; Kaviraj et al. 2007). In addition, the UV can provide reliable measures of SFR for galaxies with weak or undetected emission lines.

The goal of this paper is to investigate the dependence of the fraction of quenched galaxies on galaxy properties and DMH mass in both the observational group catalogue and several different semi-analytic galaxy formation models. Another new aspect of our study with respect to previous comparisons (e.g. Weinmann et al. 2006b) is that we compare with the results from three independently developed semi-analytic codes, and for one of the codes, we examine three different variants with different physical ingredients. In this way, we investigate how these empirical results can constrain the input physics in these kinds of models. An outline of the rest of our paper is as follows: in Section 2, we describe the empirical data sets and the group catalogues used in our study; in Section 3, we describe the theoretical models; in Section 4, we present the results of our comparisons between the empirical data and the models and we discuss our results and conclude in Section 5.

2 THE DATA SAMPLE

2.1 The SDSS group catalogue

We make use of the Galaxy group catalogue of Y07. The catalogue was constructed by applying the halo-based group finder of Yang et al. (2005) to the New York University Value-Added Galaxy Catalogue (NYU-VAGC, Blanton et al. 2005a), which is based on the Sloan Digital Sky Survey (SDSS) DR4 (Adelman-McCarthy et al. 2006). From the main Galaxy sample, Y07 selected galaxies with extinction-corrected r-band apparent magnitude brighter than $r = 17.77$, within a redshift range $0.01 < z < 0.2$, and with a redshift completeness $\mathcal{C} > 0.7$. They augmented this sample with 7091 galaxies with $0.01 < z < 0.2$ with redshifts from alternate sources. The resulting sample (sample II of Y07) has a mean redshift of $z \sim 0.1$ and a total sky coverage of 4514 deg^2, and contains 369 447 galaxies. In this paper, we refer to this as 'the SDSS sample'.

All absolute magnitudes are k- and evolution (e) corrected to the $z = 0.1$ rest frame as described by Blanton et al. (2003). Stellar masses are computed using the relation between rest-frame optical colour and mass-to-light ratio of Bell et al. (2003), as specified in Y07, assuming a Kroupa IMF. Our sample is not volume limited, and we therefore attempt to correct for the resulting Malmquist bias by weighting each galaxy by a standard $V_{\rm max}$ correction (Schmidt 1968).

The group finder first identifies a potential group centre by the friends-of-friends algorithm (Davis et al. 1985), and then computes the characteristic luminosity of each tentative group. The characteristic group luminosity is defined as the (incompleteness corrected; see Y07) combined luminosity of all group members with ${}^{0.1}M_r \leq -19.5 + 5\log h$. The characteristic group stellar mass is similarly the incompleteness-corrected total stellar mass contributed by galaxies with ${}^{0.1}M_r \leq -19.5 + 5\log h$. Then, the velocity dispersion and the virial radius of the DMH associated with each tentative group are estimated iteratively, assuming a constant mass-to-light ratio as an initial guess. These two estimates can be used for determining the spherical Navarro, Frenk & White (1997, hereafter NFW) type dark matter profile. Assuming a Gaussian probability distribution along the redshift direction and a projected spherical NFW dark matter profile for the perpendicular plane, group members are updated until there is no change in their memberships.

Lastly, a DMH mass is assigned to each group, assuming a one-to-one correlation between the characteristic stellar mass for each group and the halo mass derived from a theoretical mass function (e.g. Warren et al. 2005). We use the halo mass estimated from stellar mass, as luminosity-based halo mass estimates may be biased differently for groups with blue versus red galaxies (Y07). Y07 find that they can assign group masses down to a lower limit of $M_{\rm halo} < 10^{11.6}\,{\rm M}_\odot\,h^{-1}$, although the completeness of the group catalogue begins to drop below unity for halo masses less than $M_{\rm halo} \lesssim 10^{13}\,h^{-1}\,{\rm M}_\odot$. The central galaxy in each group is identified as the galaxy with the largest stellar mass.

There are 204 813 groups in the resulting group catalogue. Note that we call all cluster 'groups' regardless of their richness or density, including groups that contain only a single member. For a more detailed description of the group finder, and the results of extensive tests of its completeness, contamination and purity, we refer interested readers to Y07.

2.2 GALEX

The GALEX data provide near-ultraviolet (NUV, effective wavelength ∼2271 Å) and far-UV (FUV, ∼1528 Å) band information (Martin et al. 2005). Of 741 deg^2 of GALEX unique imaging, 645 deg^2 overlaps with the SDSS DR4 spectroscopic area. We make use of the GALEX–SDSS matched sample constructed by S07. S07 first define a SDSS parent sample in the GALEX overlap region of objects spectroscopically classified as galaxies, and having optical magnitude $14.5 < r_{\rm petro} < 17.77$ and redshift $0.005 < z < 0.22$. This sample contains 49 346 galaxies. For each of the galaxies in the SDSS parent sample, S07 searched within a 4 arcsec radius (corresponding to ∼7 kpc at z∼0.1) for a match in the GALEX source catalogue.

Using a large library of model Spectral Energy Distributions (SEDs) based on the Bruzual & Charlot (2003) population synthesis code, S07 then performed Bayesian SED fitting to the seven-band photometry (*FUV*, *NUV*, *u*, *g*, *r*, *i* and *z*) to obtain estimates of dust extinction, stellar mass and SFR. These parameters were built from probability distribution functions, thus taking into account parameter degeneracies. The typical error in the SSFR (obtained from the width of the SED fitting probability distribution) is 0.2 (star-forming galaxies) to 0.7 dex (passive galaxies).

Of the full S07 sample, we use 32 787 galaxies that are associated with SDSS galaxies in our group catalogue, and exclude a small number of objects with very poor fits (see discussion in section 4.3 in S07). The redshift range for this final sample is $0.01 \leq z \leq 0.2$ with mean redshift ∼0.104, and the redshift distribution is very similar to that of the parent SDSS sample.

3 THEORETICAL MODELS

We adopt a semi-analytic approach to model galaxy formation within the Λ cold dark matter picture. We make use of a total of five sets of models based on different prescriptions for our comparison with the empirical data. Three of the models are constructed using the latest version of the Somerville code (Somerville & Primack 1999; Somerville et al. 2001; S08). The others are the Millennium models (Croton et al. 2006; De Lucia et al. 2006, hereafter dL06) and the MORGANA (MOdel for the Rise of GAlaxies aNd Active nuclei) models (Fontanot et al. 2006, 2007; Monaco et al. 2007).

We describe the basic scheme in the Somerville code. We use an *N*-body simulation box to obtain the masses and positions of the 'root' DMHs, and compute the merger history for each halo using the method of Somerville & Kolatt (1999). Within each DMH, gas cools via atomic cooling (White & Frenk 1991; Somerville & Primack 1999) and forms a rotationally supported disc. The radial sizes of discs are computed using the model described in Somerville et al. (2008a), which accounts for the initial Navarro–Frenk–White profiles of the DM haloes and the 'adiabatic contraction' due to the self-gravity of the infalling baryons. Cold gas is turned into stars in the galactic disc following the Schmidt–Kennicutt law (Kennicutt 1989, 1998), and gas with surface density lower than a critical threshold density (e.g. Martin & Kennicutt 2001) does not form stars. Massive stars explode as supernovae and reheat the cold gas. We trace chemical evolution using a simple 'effective yield' parameter. Each generation of stars produces a fixed 'yield' of metals, which are deposited in the cold gas. This gas may then be ejected and mixed with the hot component by supernova or AGN-driven winds.

When a satellite is subsumed into a larger DMH, it is assumed that it immediately loses its hot gas halo, and thus does not receive any new supply of cold gas. The orbital decay and eventual merging, due to dynamical friction, of satellite galaxies within DMHs is tracked using a modified version of the Chandrasekhar (1943) formula (Boylan-Kolchin, Ma & Quataert 2008). Mass loss and tidal destruction are also accounted for, using a simplified version of the approach presented in Taylor & Babul (2004) and Zentner & Bullock (2003). Galaxy mergers trigger bursts of star formation, the efficiency and time-scales of which are modelled using results from hydrodynamic simulations of galaxy–galaxy mergers.

The code also tracks the growth of black holes and the energy they produce. Every top level DM halo is seeded with a black hole of $\sim 100\,{\rm M}_\odot$. Mergers trigger the 'bright-mode' black hole growth that is associated with luminous quasars. Following every merger with mass ratio greater than 1:10, the black hole grows at its Eddington rate until it reaches a critical mass. The critical mass is that at which the energy radiated by the black hole is sufficient to halt further accretion, i.e. the black hole growth is self-regulated (Hopkins et al. 2007). Soon after reaching the critical mass, the black hole enters a 'blowout' phase, resulting in a decline in the accretion rate. The associated radiation can also drive winds that remove cold gas from the galaxy (see S08 for details).

The S08 models also incorporate 'radio-mode' feedback associated with low-efficiency accretion. The accretion rate is computed using the isothermal Bondi flow model of Nulsen & Fabian (2000). In the presence of a quasi-hydrostatic shock-heated gas halo, the energy from this accretion is assumed to drive radio jets that can heat the gas and partially or completely offset the cooling flow.

The resulting star formation and enrichment histories are convolved with the stellar population models of Bruzual & Charlot (2003) to compute magnitudes and colours. We have adopted a Chabrier IMF. The impact of dust extinction is modelled using an analytic model, as in De Lucia & Blaizot (2007).

The S08 *fiducial model* includes all of these mechanisms. We also consider a 'no-AGN-feedback model', which does not include either the bright- or radio-mode AGN feedback mechanisms, and the 'halo-quenching' model, in which cooling is shut off when a halo grows more massive than $\sim 10^{12}\,{\rm M}_\odot\,h^{-1}$ (see Table 1 for a summary of all models). The halo-quenching model is included as an illustration of a quenching mechanism that has a simple dependence on halo mass only. A similar model has been considered by Cattaneo et al. (2006). It is based on the ideas proposed by Birnboim & Dekel (2003) and Dekel & Birnboim (2006), who suggest that whenever a halo grows above this critical quenching mass, the gas is shock heated to near the virial temperature, and can be easily kept hot by either an AGN or other processes such as heating by gas clumps or orbiting satellites (Dekel & Birnboim 2008; Khochfar & Ostriker 2008).

We also consider two additional models from other groups in this study. The dL06 models contain similar ingredients to the S08 models, with the following differences. They are based on merger trees extracted from the Millennium *N*-body simulations (Springel et al. 2005). Unlike in the models of S08, they do not include the effects of adiabatic contraction and an NFW halo profile in their estimates of galaxy sizes, which lead to a different evolution in the SFRs and gas fractions in their models. They use somewhat different (though similar in spirit) recipes for star formation and supernova feedback, and they use a different approach for modelling black hole growth (though, like S08, they assume that 'bright-mode' black hole growth is triggered by mergers). They do not include 'bright-mode' AGN feedback (AGN-driven winds), and their treatment of the

Table 1. Model descriptions.

Model	Box size (Mpc h^{-1})	Characteristics
S08 AGN-feedback (fiducial)	120	Bright-mode AGN-driven winds + radio-mode AGN heating
S08 no-AGN-feedback	120	Control model without AGN feedback
S08 HQ	120	Cooling quenched according to the halo mass
dL06	120	Radio-mode AGN heating
MORGANA	144	Bright-mode AGN-driven winds + Radio-mode AGN heating

radio-mode feedback is again similar in spirit but different in detail from S08. Magnitudes and colours (including dust extinction) are computed in a similar manner to S08, and use a Chabrier IMF. We obtained the dL06 catalogues from the public Millennium data base (http://www.g-vo.org/Millennium).

We also consider the predictions of the semi-analytic model MORGANA (Fontanot et al. 2006, 2007; Monaco et al. 2007). MORGANA follows a scheme similar to S08 and dL06, but it includes a different treatment for the thermal processes acting on baryonic gas. More details on the updated version we use in this paper are presented in Lo Faro et al. (in preparation). The model is based on merger trees obtained using the PINOCCHIO method (Monaco, Theuns & Taffoni 2002), similar to those predicted by *N*-body simulations. Gas cooling and infall follow the prescription described and tested in Viola et al. (2008), while star formation and stellar feedback are then modelled as in Monaco (2004). When two DM haloes merge, dynamical friction, tidal stripping and tidal shocks on the satellite galaxies are followed using the Taffoni et al. (2003) formulation. Similarly to S08, when a satellite DM halo merges into a larger one, all of its hot gas is shock heated according to the new halo potential and gets removed from the satellite (thus implying that the corresponding satellite galaxy does not receive any further cold gas supply). Disc sizes are computed using the model of Mo, Mao & White (1998), and bulge sizes are computed assuming that kinetic energy is conserved in mergers.

A key ingredient in MORGANA is the inclusion of a self-consistent model for the accretion of gas on to supermassive black holes and the resulting AGN feedback modes (following Umemura 2001 and Granato et al. 2004, see Fontanot et al. 2006 for more details). This modelling assumes that the loss of angular momentum is the main regulator of black hole accretion. This is triggered by the presence of gas in the bulge component, and the almost complete loss of angular momentum of accreted gas is related to star formation activity. Following Granato et al. (2004), star formation creates a reservoir of low angular momentum gas which is then accreted at a rate regulated by the viscous accretion time-scale or the Eddington limit. The nature of feedback from the AGN depends on the accretion rate in Eddington units: whenever this is higher than 0.01 ('bright mode'), the AGN can trigger a massive galactic-scale wind (see Monaco & Fontanot 2005) which leads to the complete removal of the ISM from the galaxy, while at lower accretion rates ('radio mode') the energy is ejected through jets that feed back on the hot halo gas with an efficiency that scales with V_c^2, where V_c is the halo circular velocity. As a consequence, BH accretion requires some star formation to be triggered, and feedback follows the onset of cooling only after some time. The ejected energy heats the hot halo gas component and quenches the cooling flow. Galaxy SEDs, magnitudes and colours are obtained using the GRASIL spectrophotometric code with radiative transfer for computing the effect of dust (Silva et al. 1998).

In Table 1, we present a brief description of each model.

4 RESULTS

In this section, we investigate the joint dependence of star formation quenching on *stellar mass* and *halo mass*, in order to try to constrain the physical mechanisms that are responsible for quenching. We make use of two indicators of quenched star formation: red optical colours and low SSFRs (SSFR $\equiv$ SFR/$M_{\rm gal}$). Red optical colours are frequently used to isolate 'quenched' galaxies; however, a red optical colour can arise from a degenerate combination of an old stellar population, a high metallicity or strong dust extinction. SSFR based on UV-optical data is a more sensitive probe of recent star formation.

In order to mimic the selection effects of the flux-limited observational sample, we first assign redshifts to all the model galaxies by placing an 'observer' in a corner of the simulation box. We apply the same flux limit used in the observational catalogues to the models by selecting only galaxies with apparent *r*-band magnitude $r < 17.77$. We then apply the $V_{\rm max}$ weighting factor, just as we do with the galaxies in the observational sample. Then, we exclude all haloes that do not contain any galaxy brighter than ${}^{0.1}M_r \geq -19.5 + 5\log h$, as these haloes would not be included in the group catalogue.

We apply these selection criteria for all of the model-data comparisons shown in the main text, unless otherwise noted. We also present our main results for the models without these selection criteria in the Appendix.

4.1 Global distribution functions: colour and SSFR

In Fig. 1, we present the global colour–magnitude relations (CMRs) at $z = 0.1$ for the observations and theoretical models, along with the dividing line between the observed red sequence and the blue cloud (sometimes called the 'green valley'). In this figure, we show the results for the whole SDSS sample, regardless of inclusion in the group catalogue, and similarly we have not applied the observational selection criteria to the theoretical models. The magnitudes and colours are shown in the rest-frame $z = 0.1$ system defined by Blanton et al. (2003). For the dL06 models, we used the observed frame magnitudes at $z = 0.1$, converted to absolute magnitudes. For the MORGANA galaxies, we compute the absolute $z = 0.1$ magnitudes from the corresponding synthetic spectra. For the S08 models, when we computed standard $z = 0.0$ frame colours and magnitudes, we produced a good match to the observed CMR expressed in the $z = 0$ frame. However, when we computed the $z = 0.1$ system colours as described in Blanton & Roweis (2007), we found it necessary to apply a shift of 0.05 mag to the ${}^{0.1}(g - r)$ colour to match the location of the observed $z = 0.1$ system red sequence. This is indicative of small differences in the shape of the SED's in the semi-analytic models from the synthetic SED's used by Blanton et al. (2003) for computing the *k*-corrections. It should also be noted that details in the population synthesis prescriptions, such as chemical enrichment

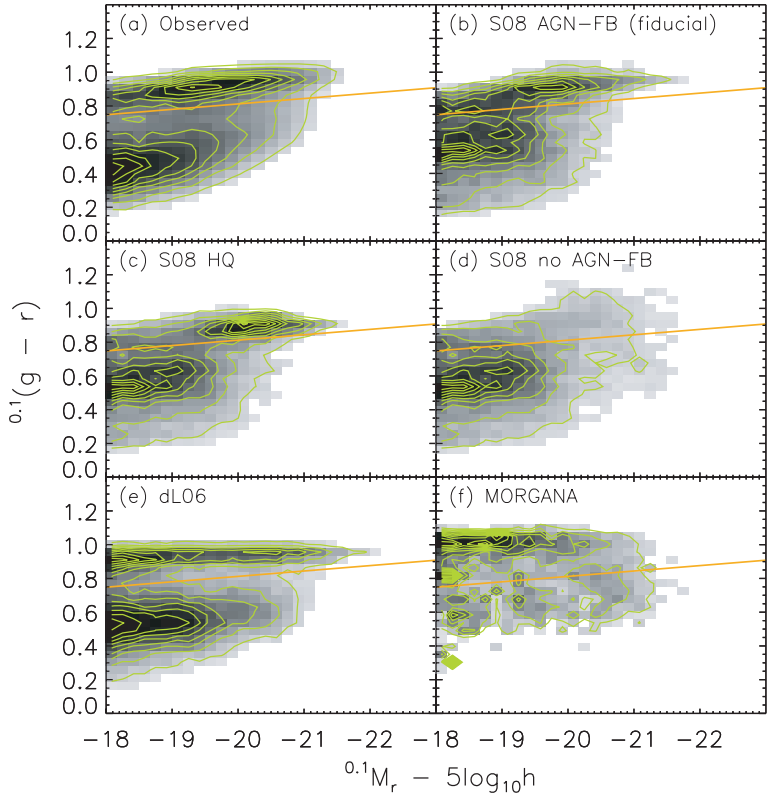

Figure 1. The distribution of $^{0.1}r$-band absolute magnitude versus $^{0.1}(g-r)$ colour. Grey shading and green contours show the conditional probability $P[^{0.1}M_r|^{0.1}(g-r)]$. The orange line shows the demarcation line for the 'red' and 'blue' galaxy populations used in this study.

and dust extinction, may also cause notable differences in colours (see Appendix for the effect of dust). Therefore, reproducing the CMR quantitatively in semi-analytic models is quite challenging.

The observations clearly show the familiar red sequence and blue cloud, and these features are reproduced reasonably well in all of the theoretical models, except the S08 no-AGN-feedback model. As has been pointed out before (e.g. Cattaneo et al. 2006; Croton et al. 2006), semi-analytic models without some kind of suppression of cooling in massive haloes, e.g. by AGN feedback, predict that massive galaxies are still accreting plenty of cold gas at the present day, and therefore are star forming and blue, in conflict with observations. We do see subtle differences in the structure of the CM distribution for the different models, for example, the S08-halo-quenching model produces very few low-luminosity red galaxies, and the dL06 model produces a very strong bimodality. Also, we note that the red sequence in the halo-quenching model is slightly bluer compared with the S08 fiducial model. This is because the central galaxies in the halo-quenching model stop forming stars once their halo becomes more massive as $10^{12}\,h^{-1}\,\mathrm{M}_{\odot}$. In general, this happens at an earlier epoch than the 'radio-mode' feedback is able to quench star formation. Because chemical evolution is also halted when star formation is quenched, the massive galaxies in the halo-quenching model do not become as enriched as do the galaxies in the fiducial model (see S08). We could have adjusted for this by increasing the chemical yield, but we chose to leave all the free parameters fixed in both models to allow a direct comparison.

The behaviour of MORGANA is somewhat different from that of the other models. A clear red sequence is present at intermediate and faint magnitudes, but it fades away at bright magnitudes, in contrast to the observations. Luminous galaxies tend to be blue. We interpret this result as an inefficient quenching of star formation through 'radio-mode' feedback in MORGANA. In fact, as explained in Section 3, in this model the AGN heating switches on only after some cooled gas has already started forming stars in the host galaxy. Obviously, the residual activity is stronger for longer time delays between the onset of cooling flows and the accretion on to the central black hole. On the other hand, the blue cloud seems depleted. As shown in Fontanot et al. (2009), the depletion of the blue cloud is connected in part to the 'satellite overquenching problem', discussed further in Section 5, caused by the too-efficient strangulation of satellite galaxies. However, we will see later that MORGANA also produces too few low-mass blue central galaxies. This is likely due to strong supernova feedback.

Given the strongly bimodal colour distribution exhibited by both the empirical data and most of the models, it is natural to define a dividing line between the two populations, and to investigate the fraction of galaxies in the red population, f_{red}, as representing quenched objects. We adopt the same demarcation line between red and blue galaxies as W06a

$$^{0.1}(g-r) = 0.7 - 0.032(^{0.1}M_r - 5\log_{10}h + 16.5) \quad (1)$$

as shown in Fig. 1.

We can also define the SSFR, as the present SFR divided by the stellar mass of the galaxy (=SFR/M_{gal}), and plot a similar diagram in terms of SSFR and mass. In Fig. 2, we show the conditional probability distribution for SSFR as a function of stellar mass, as derived from the GALEX + SDSS observations, and for the models. The SFR is averaged over the past 100 Myr. Note that the number of galaxies in the sample is roughly eight times smaller than the sample shown in the CM distribution plot, because the field coverage of

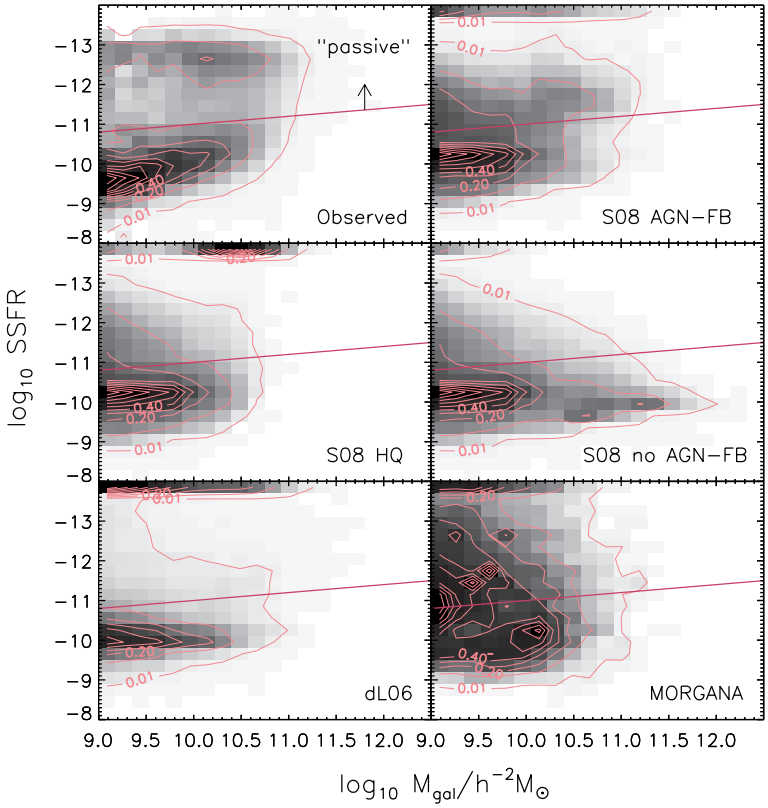

Figure 2. Galaxy stellar mass versus SSFR. Grey shading and pink contours show the conditional probability $P(M_{\rm gal}|{\rm SSFR})$. The purple line shows the demarcation line between 'passive' and 'active' galaxies used in this study.

GALEX survey used in the Salim et al. study is not as wide as that of the SDSS. In a similar manner, we define a cut in SSFR to separate 'active' star-forming galaxies from 'passive' ones. We define a galaxy as 'passive' if the following condition is met:

$$\log_{10}{\rm SSFR} \leq -9 - 0.2\log_{10}(M_{\rm gal}/h^{-2}\,{\rm M}_{\odot}). \quad (2)$$

Note here that our criterion is based on galaxy stellar mass in order to make a more direct comparison with the theoretical models. It is also worth noting that our criterion roughly corresponds to SFR $\sim$1 $\mathrm{M}_{\odot}\,\mathrm{yr}^{-1}$ at $M_{\rm gal} \sim 10^{11}\,h^{-2}\,\mathrm{M}_{\odot}$ and SFR $\sim 0.1\,\mathrm{M}_{\odot}\,\mathrm{yr}^{-1}$ at $M_{\rm gal} \sim 10^{9.5}\,h^{-2}\,\mathrm{M}_{\odot}$. Below $0.1\,\mathrm{M}_{\odot}\,\mathrm{yr}^{-1}$, SFR obtained from multiband photometry may not be robust due to the degeneracy of burst time and the mass fraction of a young population (e.g. Kaviraj et al. 2007).

Our demarcation is comparable to that of W06a when their criterion, which is based on the $^{0.1}r$-band magnitude, is lowered by 0.6 dex. However, SFR estimates from emission lines, which were used by W06a, trace only very recent star formation, whereas the UV used here traces star formation over a longer time-scale ($\sim$1 Gyr). Therefore, our 'passive' sample is not directly comparable to that of W06a, though the results are qualitatively similar. The amount of UV flux in the passive galaxies is very small and can still be consistent with the amount of UV flux that can be produced by old stars such as low-mass horizontal-branch stars (see Yi et al. 2005 for details). In this regard, it is justifiable to call them 'passive'.

In Fig. 2, we see a well-defined 'star-forming sequence' that produces the blue sequence in the traditional CM diagram, but the 'quenched' population that produces the tight red sequence is quite spread out in SSFR. This is simply a reflection of the relative insensitivity of optical colours to small amounts of recent star formation. The precise values of SSFR at low levels of star formation cannot be estimated very accurately from the data, and therefore one should not take too seriously the position of the quenched galaxies in the SSFR versus $M_{\rm gal}$ plot. Again, the models with AGN feedback (or halo quenching) qualitatively reproduce the empirical distribution reasonably well, but show some interesting differences. The dL06 model has a strongly bimodal distribution of SSFR, with most galaxies living either on the star-forming sequence or being completely quenched. In contrast, the S08 model has a larger population of 'semi-quenched' galaxies at intermediate values of SSFR. The MORGANA model produces an even broader distribution of SSFR, with many quenched low-mass galaxies.

4.2 Dependence of star formation quenching on stellar mass

Fig. 3 shows the dependence of $f_{\rm red}$ and $f_{\rm passive}$ on galaxy stellar mass. We show $f_{\rm red}$ and $f_{\rm passive}$ versus stellar mass for all galaxies (upper panels), and for central and satellite galaxies separately (middle and lower panels, respectively). Although we do not specifically use the information from the group catalogue in the uppermost panel, in all panels we use only the SDSS galaxies that are included in the group catalogue, and apply the group catalogue-like selection criteria to the theoretical models, as described at the beginning of this section.

In the empirical data, $f_{\rm red}$ shows a strong dependence on galaxy mass for both centrals and satellites, in the well-known sense that low-mass galaxies are largely blue, whereas massive galaxies are more likely to be red. It appears that $f_{\rm red}$ is a steeper function of stellar mass for central galaxies than for satellites. In general, the red galaxy fraction is higher for satellites for a fixed galaxy mass. Similarly, van den Bosch et al. (2008a,b) found that satellite galaxies

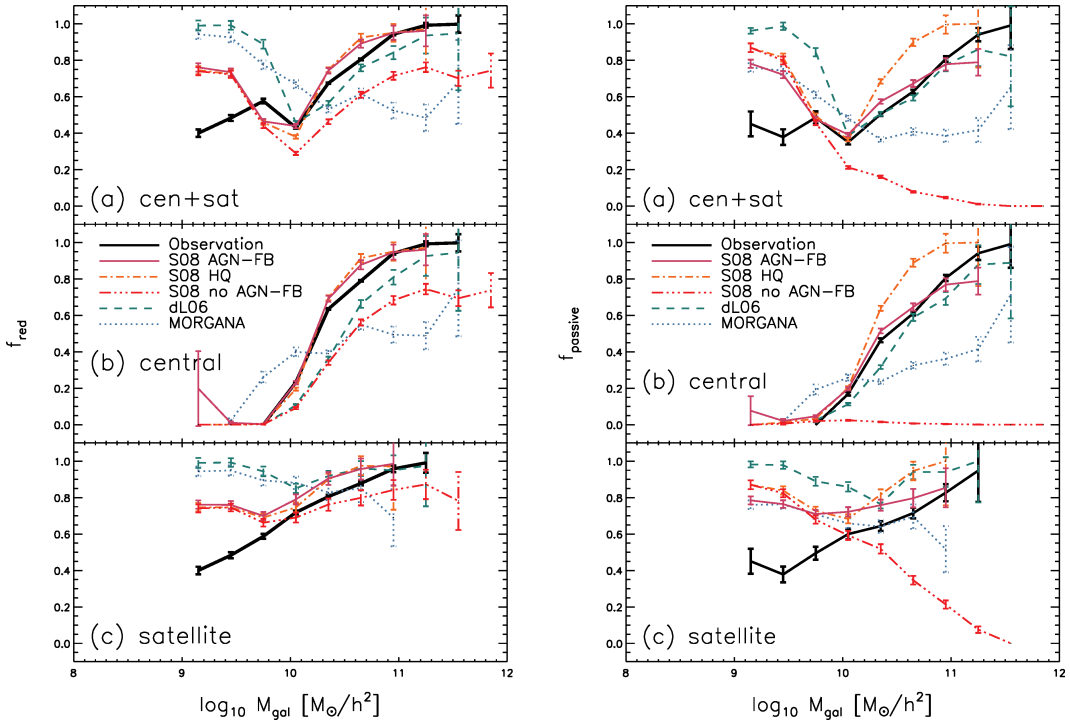

Figure 3. The fraction of red galaxies ($f_{\rm red}$; left-hand panel) and passive galaxies ($f_{\rm passive}$; right-hand panel) as a function of galaxy stellar mass. The empirical data are shown by a black solid line, and coloured lines show the results of the theoretical models, as indicated on the plot. We show the dependence for all galaxies (top panel), central (middle panel) and satellite (bottom panel) galaxies separately. Each point contains at least 10 galaxies. Most of the Semi-Analytic Models (SAMs) reproduce the trend for central galaxies reasonably well, but predict a much larger fraction of small-mass red/passive satellite galaxies than are observed. The error bars indicate Poisson errors.

have redder mean colours than centrals at a fixed stellar mass. The trends appear qualitatively very similar when we consider $f_{\rm passive}$ as a function of stellar mass.

The S08 fiducial model, S08-halo-quenching model, and dL06 model all reproduce the trends in $f_{\rm red}$ and $f_{\rm passive}$ with stellar mass quite well for *central* galaxies. Note the similarity of the predictions of the S08 fiducial and halo-quenching model. The S08 no-AGN-feedback model, as we have already seen, predicts the presence of too many massive blue central galaxies. MORGANA reproduces the sense of the trend of the red fraction with stellar mass, but slightly overproduces red galaxies at low stellar masses, and significantly overproduces blue galaxies at high stellar masses.

All of the models badly overproduce the number of low-mass red satellites, and predict too weak a trend of $f_{\rm red}$ with stellar mass for these objects. The dL06 models predict a nearly flat run of $f_{\rm red}$ with stellar mass for satellites, with values that are much too high (close to unity) compared with the empirical values. At the highest satellite masses, there is *too high* a fraction of blue galaxies in the MORGANA model and the S08 no-AGN-feedback model. We can see by comparing the S08 no-AGN-feedback model with the fiducial model that AGN feedback does not affect galaxy colours below stellar masses of $\sim 10^{10}\,h^{-2}\,{\rm M}_{\odot}$; therefore, *the excess of low-mass red satellites is not connected with AGN feedback.*

The conclusions we would draw from the comparison with $f_{\rm passive}$ are qualitatively similar, though quantitatively somewhat different. For example, the dL06 model shows a better quantitative match to the $f_{\rm passive}$ data than to $f_{\rm red}$ for central galaxies. The S08 fiducial and halo-quenching models produced almost indistinguishable results for $f_{\rm red}(M_{\rm gal})$, but significantly different results for $f_{\rm passive}(M_{\rm gal})$. This is due to the age–metallicity degeneracy – as we discussed in Section 4.1, massive galaxies in the halo-quenching model are more metal poor than in the fiducial model. Therefore, although they are older (as seen in the $f_{\rm passive}$ diagram), their optical colours are similar. Similarly, the large difference between $f_{\rm red}$ and $f_{\rm passive}$ for the S08 no-AGN-feedback model is due to dust extinction: in this model, massive galaxies are actively star forming, and therefore extremely dusty (see Appendix for more discussion of the effects of dust extinction).

The somewhat lower fraction of red/passive satellite galaxies in the S08 models is due to the inclusion of tidal destruction, which is not included in the dL06 or MORGANA models. In the S08 model, satellites that orbit within their host halo for a long time can eventually become tidally destroyed, and their stars are added to a 'diffuse stellar halo' (see S08). Naturally, in the absence of tidal destruction, these satellites exhaust all of their gas and become very red. However, we see here that although the inclusion of tidal destruction helps us to reduce the excess of low-mass red satellites in the models, a significant discrepancy still remains.

One might then wonder whether increasing the efficiency of tidal destruction could completely solve the satellite 'overquenching' problem that we see here. We do not believe that this is a viable solution, for several reasons. First, the tidal disruption model used by S08 was tuned to match the substructure mass function for very high resolution *N*-body simulations. S08 also showed that their models correctly reproduce the total number of low-mass galaxies (i.e. the faint-end slope of the stellar mass function), although the model overproduces low-mass bulge-dominated (red/passive) galaxies and underproduces low-mass disc-dominated (blue/active) galaxies. Significantly increasing the efficiency of tidal destruction would be in conflict with the *N*-body results and would also

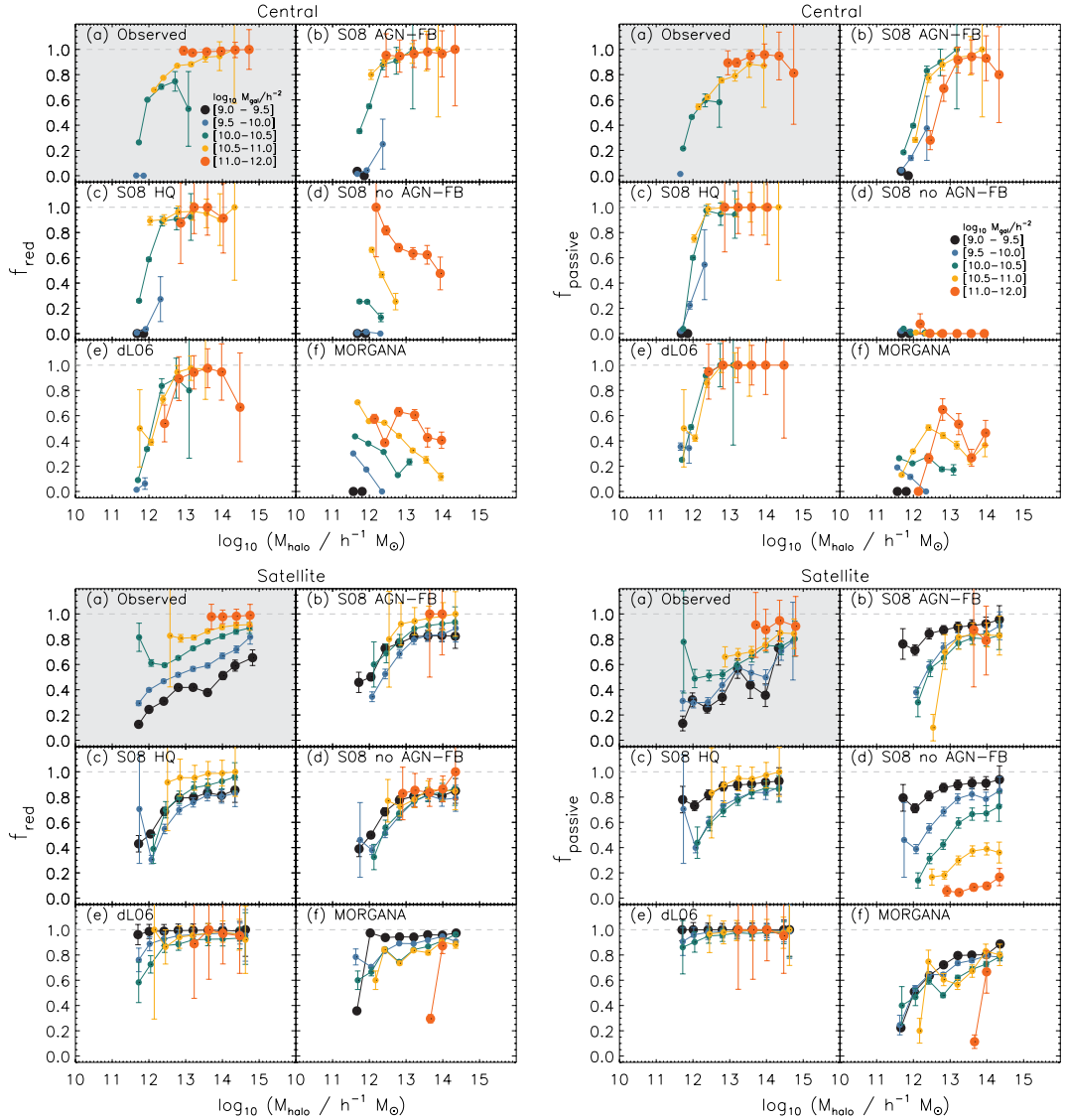

Figure 4. The red fraction f_{red} (left-hand panel) and passive fraction $f_{passive}$ (right-hand panel) as a function of halo mass, for different stellar mass bins, as indicated by different colours and symbol sizes (see plot legend). In each plot, results are shown for the observed SDSS or GALEX + SDSS group catalogue (top left-hand panel) and the five models as indicated on the plot. We present the results for central (top set of panels) and satellite (bottom set of panels) galaxies separately. Each point contains at least five galaxies. The SAMs reproduce the main trends reasonably well for central galaxies, but satellite galaxies do not show the correct trend of f_{red} with stellar mass.

produce an overall deficit of low-mass galaxies. Put another way, tidal destruction can remove low-mass red satellites but cannot increase the number of low-mass blue satellites.

4.3 Dependence on stellar mass and halo mass

In this section, we explore the dependence of f_{red} and $f_{passive}$ on DM halo mass and stellar mass. In Fig. 4, we show f_{red} and $f_{passive}$ as a function of halo mass, for different bins in stellar mass. We show the results for f_{red} and $f_{passive}$ for central galaxies (top row), and for satellite galaxies (bottom row). In Fig. 5, we show a similar plot, but this time with the galaxy stellar mass plotted on the x-axis, and different bins in halo mass shown by the different colours.

In the empirical data, we see that for massive $M_{gal} > 10^{11}\,h^{-2}\,M_\odot$ *central* galaxies, there is no significant dependence of f_{red} on halo mass (environment) for fixed stellar mass. For intermediate-mass galaxies ($10^{10}\,h^{-2} < M_{gal} < 10^{11}\,h^{-2}\,M_\odot$), the dependence on halo mass appears to be stronger, but there is a limited region of overlap in galaxies with different stellar masses that occupy haloes of the same mass. This is because there is a fairly tight correlation between halo mass and stellar mass. Similar results are again obtained for $f_{passive}$.

The S08 fiducial and dL06 models, both of which include AGN feedback, do reasonably well at reproducing the overall trends for central galaxies, as does the S08-halo-quenching model. We see a hint of a dependence on stellar mass in intermediate-mass haloes ($10^{11.5} \lesssim M_{halo} \lesssim 10^{12.5}\,h^{-1}\,M_\odot$) in the S08 models, while in the dL06 model, the dependence seems to be almost solely on halo mass. However, interestingly, we see almost the same stellar mass dependence in the S08 fiducial and halo-quenching models, while we know that the quenching mechanism is a pure function of halo mass in the halo-quenching model. The S08 no-AGN-feedback model

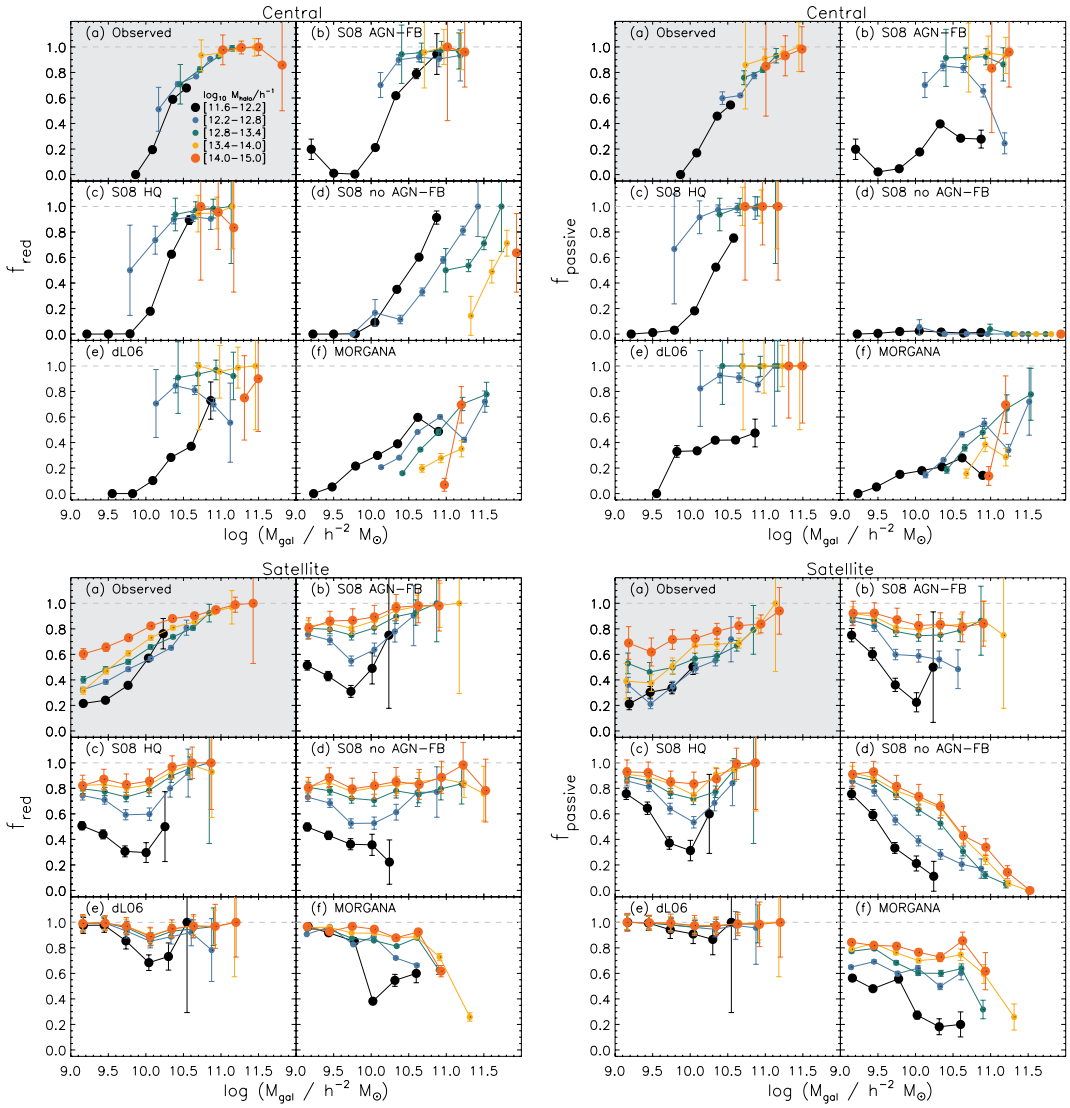

Figure 5. The red fraction $f_{\rm red}$ (left-hand panel) and passive fraction $f_{\rm passive}$ (right-hand panel) as a function of stellar mass, for different halo mass bins, as indicated by different colours and symbol sizes (see plot legend). The rest of the plot details is as in Fig. 4.

shows the correct trend with stellar mass at fixed halo mass (more massive galaxies have higher $f_{\rm red}$), but the opposite trend with halo mass (more massive haloes have lower $f_{\rm red}$). Interestingly, MORGANA shows similar trends to the S08 no-AGN-feedback model: this implies that the current implementation of AGN feedback in this model is insufficient to fully cure the 'star formation quenching' problem.

Considering $f_{\rm passive}$, we see somewhat different behaviour. The S08 no-AGN-feedback model produces no quenched galaxies at all in terms of $f_{\rm passive}$. The S08 and dL06 models appear surprisingly similar, both showing almost a pure halo mass dependence (no significant dependence on stellar mass). On the other hand, MORGANA predicts a significant dependence of $f_{\rm passive}$ on stellar mass, while showing overall low values of $f_{\rm passive}$.

Observed satellite galaxies show an $f_{\rm red}$ dependence that is very similar to that of centrals for massive galaxies ($M_{\rm gal} \gtrsim 10^{10.5}\,h^{-2}\,{\rm M}_{\odot}$). For intermediate- and low-mass satellites, $f_{\rm red}$ shows some dependence on both galaxy stellar mass and halo mass, but does not show the very sharp drop over intermediate halo masses ($11.5 \lesssim M_{\rm halo} \lesssim 12.5\,h^{-1}\,{\rm M}_{\odot}$) seen in the central population. In the semi-analytic models, we see that $f_{\rm red}$ for the satellites does not have a strong enough dependence on $M_{\rm gal}$ at fixed halo mass.

The stellar mass dependence of $f_{\rm passive}$ for satellites in the empirical sample is not as clear as it was in terms of $f_{\rm red}$. This may be, in part, due to the smaller size of the GALEX–SDSS matched sample used to obtain $f_{\rm passive}$. The S08 models now all show a clear *inverted* trend: $f_{\rm passive}$ is higher for lower mass galaxies (the opposite of the empirical trend). For the dL06 model, nearly all satellites are passive regardless of their stellar mass or halo mass. In MORGANA, satellite properties are a weak function of stellar mass, and the values of $f_{\rm passive}$ are overall too high.

Based on Fig. 4 alone, we might be tempted to conclude that quenching is primarily a function of halo mass. However, Fig. 5 shows that quenching could equally well be considered to be primarily a function of stellar mass. We conclude that, especially for central galaxies, the degeneracy between stellar mass and halo mass is too strong to reach a firm conclusion on this point.

In Fig. 6, we present the $f_{\rm red}$ and $f_{\rm passive}$ distributions in the ($M_{\rm halo}$, $M_{\rm gal}$) plane. We pixelize the ($M_{\rm halo}$, $M_{\rm gal}$) plane, compute $f_{\rm red}$ and

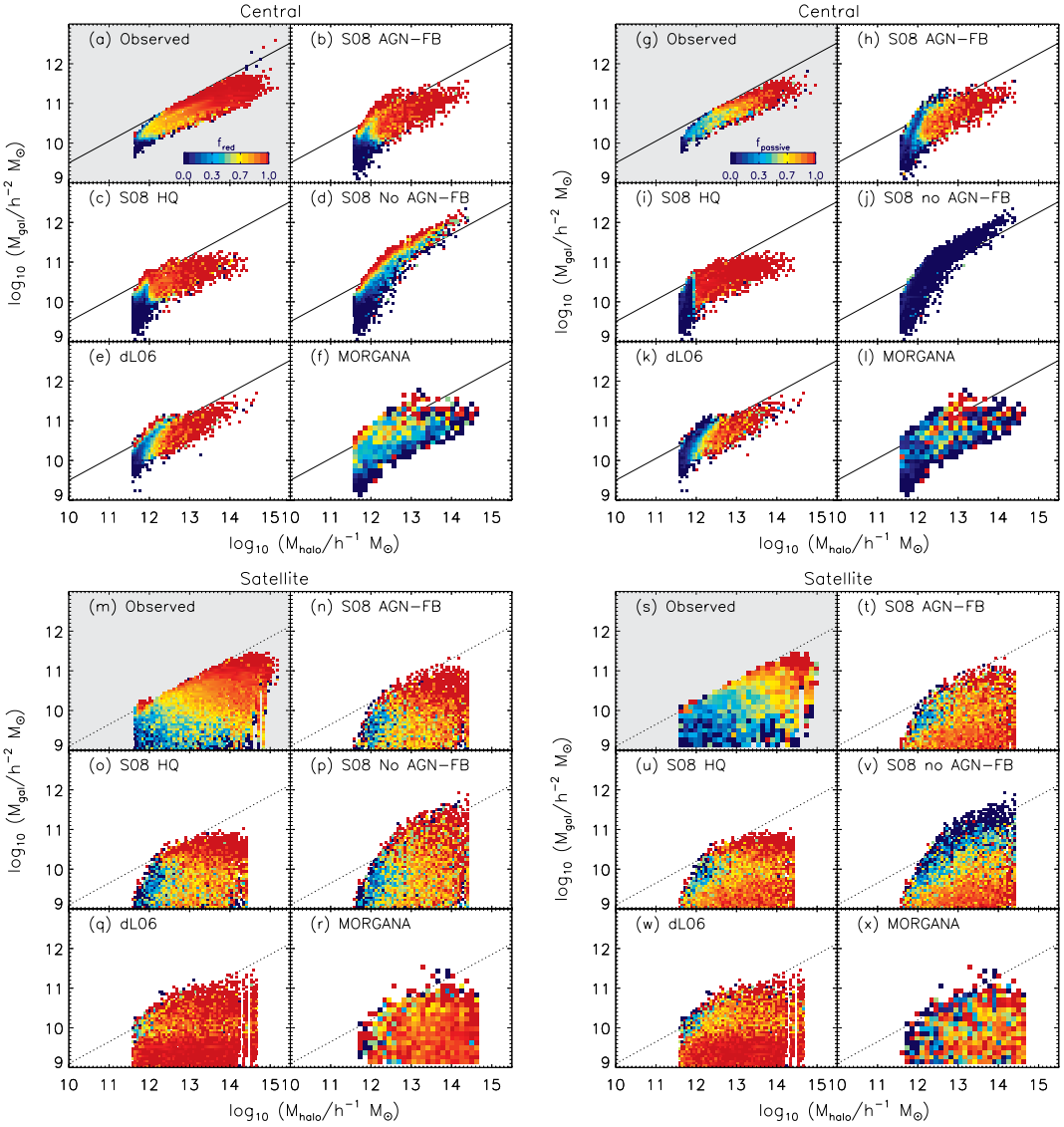

Figure 6. The fraction of 'red' galaxies ($f_{\rm red}$; left-hand panel) and passive galaxies ($f_{\rm passive}$; right-hand panel) for central (top set of plots) and satellite (bottom set of plots) galaxies in the $(M_{\rm halo}, M_{\rm gal})$ plane. The fraction of red/passive galaxies in a given pixel in $(M_{\rm halo}, M_{\rm gal})$ is indicated by the colour, where red colours indicate a higher red/passive fraction, as shown in the scale. To guide the eye, we draw a solid (dotted) line showing the approximate upper envelope of the central (satellite) galaxy mass distribution for the observational group catalogue, and repeat this same line on every panel. Central and satellite galaxies in the observational group catalogues show notably different joint dependencies on stellar mass and halo mass. The models with AGN feedback qualitatively reproduce the trends for central galaxies, but do not reproduce the empirical trends for satellites.

$f_{\rm passive}$ in each pixel, and indicate its value by the colour of the pixel. For example, a red colour indicates that galaxies are mostly red or passive within the pixel, while a blue colour indicates that most of the galaxies are blue/active. These diagrams reveal a number of interesting features. Considering the diagram for central galaxies in the empirical sample, we see that above a critical halo mass ($M_{\rm halo} \gtrsim 10^{13}\,h^{-1}\,{\rm M}_\odot$), nearly all galaxies are red and passive. For intermediate halo masses $10^{11} \lesssim M_{\rm halo} \lesssim 10^{13}\,h^{-1}\,{\rm M}_\odot$, the structures show a complex dependence on both halo mass and stellar mass. In particular, we note that above a 'critical' stellar mass of 2–3 $\times\ 10^{10}\,h^{-2}\,{\rm M}_\odot$, the majority of galaxies are red and passive, regardless of their halo mass (though such massive galaxies are not found in haloes less massive than $10^{12}\,h^{-1}\,{\rm M}_\odot$). Comparing with the models that showed good qualitative behaviour in terms of the binned quantities (S08 fiducial, S08 halo quenching and dL06), we can see that the distribution of the patterns in ($M_{\rm halo}$, $M_{\rm gal}$) space is quite different from the observations – in general, the structures show stronger vertical divisions, indicating a stronger dependence on halo mass than on galaxy mass. It is interesting to note that these three models look much more similar to one another than any of the models does to the empirical data. It is also interesting that in terms of $f_{\rm red}$, the S08 fiducial and S08-halo-quenching models look very similar to one another, but they look extremely different in the $f_{\rm passive}$ diagram. This again illustrates that optical colours are not an ideal probe of star formation quenching.

The observed satellites show an interesting striation, which is nearly horizontal at the highest and lowest stellar masses, but somewhat diagonal for intermediate masses. It appears that the majority of satellite galaxies are red/passive if they are more massive than a few times $10^{10}\,h^{-2}\,{\rm M}_\odot$ (just as for the central population),

and are predominantly blue/active if they are less massive than $10^{10}\,h^{-2}\,\mathrm{M}_{\odot}$, regardless of their halo mass. For intermediate halo masses, it seems that unlike for central galaxies, the critical mass that marks the transition between mostly blue and mostly red galaxies *is a function of halo mass*, and lower for higher halo masses. This suggests that the star formation activity in the most massive satellites is regulated by the same processes that shape centrals, while lower mass satellites are influenced by environmental processes such as tidal forces or ram pressure stripping.

All the models fail quite miserably to reproduce the satellite properties. In addition to simply predicting too high a fraction of red satellites, none of the models shows the diagonal pattern of contours in the $f_{\rm red}$ or $f_{\rm passive}$ diagrams. The few pixels with high blue fractions in the models lie at high stellar mass for their halo mass, which is the opposite from what is seen in the empirical data. These are simply galaxies that were forming stars as centrals and have become satellites very recently.

Readers are referred to the Appendix for a discussion of the impact on our results of the modelling of dust extinction, our imposed selection criteria and possible biases in the procedure for assigning halo masses in the SDSS group catalogue.

4.4 Connection with morphology, black hole formation and AGN feedback

These results naturally beg the question: which physical process(es) are responsible for imprinting this dependence of star formation quenching on galaxy and halo mass? Although this is a complex question that we will not be able to fully address in this paper, we attempt to at least identify some promising hypotheses that can be pursued further in the future.

As already discussed by many authors (e.g. Kauffmann et al. 2003), we are suspicious that the correlation of star formation quenching with stellar mass may in fact be linked to the tendency of the *increasing bulge fraction* also with stellar mass and perhaps halo mass. Although we have only rough morphological information for SDSS, we make use of a standard cut in concentration index ($C \equiv r_{90}/r_{50}$) to coarsely divide our sample into early- and late-type galaxies (early types have $C > 2.6$; Shimasaku et al. 2001; Strateva et al. 2001). Such classification using the concentration index is subject to contamination at roughly the 20 per cent level (Strateva et al. 2001). We then plot $f_{\rm early}$ in the ($M_{\rm halo}$, $M_{\rm gal}$) plane as before,[1] and show the results in Fig. 7. We see a strikingly similar pattern to the one seen when we plotted $f_{\rm red}$ and $f_{\rm passive}$ in this way in Fig. 6, indicating a very strong correlation between red, passive and early-type galaxies.

We test the connection of black hole mass with star formation quenching by plotting the ratio of black hole mass to the total stellar mass of the galaxy ($\langle M_{\rm BH}/M_{\rm gal}\rangle$) in the same ($M_{\rm halo}$, $M_{\rm gal}$) plane, which we do in Fig. 8 (for central galaxies only). Note that all three semi-analytic model codes reproduce the empirical relation between bulge mass and black hole mass reasonably well within the observational errors. In the S08, dL06 and MORGANA models, we see that the galaxies that have the *highest* stellar mass to halo mass ratios have the *lowest* black hole mass to stellar mass ratios. This is a reflection of the spread in halo merger histories at fixed halo mass. In haloes in which a massive black hole is formed relatively early, the cooling flow is also shut off at an earlier time, halting further galaxy growth except by mergers. Conversely, haloes with relatively small black holes for their mass will be able to continue to cool, and the central galaxies will continue to form stars and remain blue. This is seen to be the case in the 'blue ridge' in Fig. 6 (see panels h, k and l). Note that neither the strong trend in $\langle M_{\rm BH}/M_{\rm gal}\rangle$ nor the 'blue ridge' is seen in the S08-'halo-quenching' model, in which quenching is regulated purely by the halo mass.

In all three models with AGN feedback, there is also a trend with halo mass in the sense that larger mass haloes have larger black-hole-to-stellar-mass ratios. This is due to the dual modes of black hole growth in the models. In the 'bright mode', the growth of the stellar bulge and the black hole is linked. Most of the black hole growth in the models occurs via this bright mode of black hole feeding. However, at late times, large mass haloes can develop a hot hydrostatic halo which is assumed to fuel the 'radio mode' of

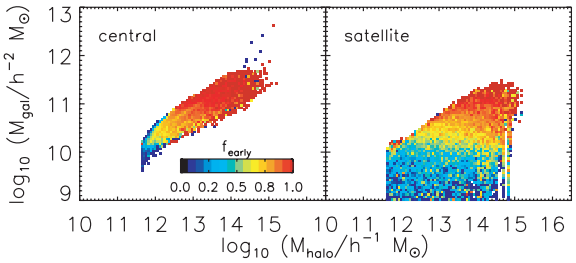

Figure 7. The fraction of early-type galaxies ($f_{\rm early}$), for centrals (left-hand panel) and satellites (right-hand panel) in the SDSS group catalogue. Early-type galaxies are defined as having a concentration index (C) greater than 2.6.

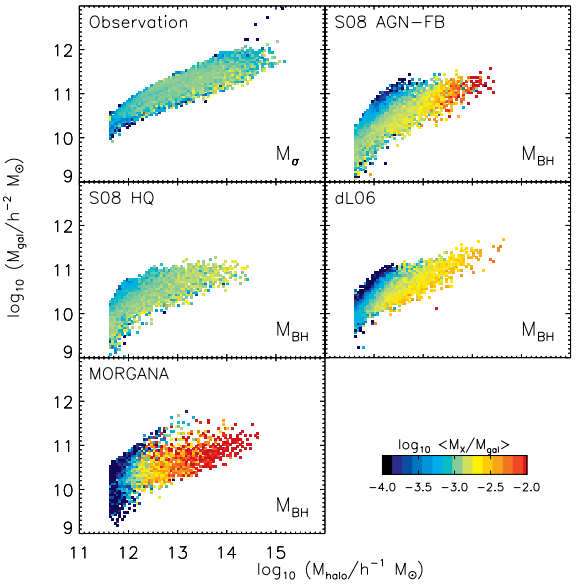

Figure 8. Average black hole mass to galaxy stellar mass ratio $\langle M_{\rm BH}/M_{\rm gal}\rangle$ for central galaxies shown by the colour coding, as a function of $M_{\rm halo}$ and $M_{\rm gal}$, for four of the theoretical models. For the S08 and dL06 models, note the similarity of the structures seen here to those seen in the plot of $f_{\rm passive}$ in Fig. 6. This suggests that for intermediate halo masses, $f_{\rm passive}$ is closely related to $\langle M_{\rm BH}/M_{\rm gal}\rangle$ in the models. We also show $\langle M_{\sigma}/M_{\rm gal}\rangle$ for the SDSS group catalogues, where M_{σ}, based on the SDSS measured velocity dispersion and the observed $M_{\rm BH}$–σ relation, is used as a proxy for the average black hole mass. Interestingly, the strong dependence of $\langle M_{\sigma}/M_{\rm gal}\rangle$ on halo mass is not visible.

[1] Because of the difficulty of mapping, the morphological information available in the models to the observable concentration index, we do not show the model predictions. The qualitative trends in the models are similar.

black hole growth. In these haloes, the black hole can grow without any associated star formation, leading to an increase in $\langle M_{\rm BH}/M_{\rm gal}\rangle$. This is supported by the fact that we do not see such a trend in the halo-quenching model, which only contains black hole growth via the bright mode.

We attempt to investigate whether this trend exists in the empirical data, using the SDSS velocity dispersion σ as a proxy for black hole mass. We compute M_σ from the $M_{\rm BH}$–$\sigma_{\rm e}$ relation using the empirical relation of Gebhardt et al. (2000). We assign a scatter to the black hole mass at a given σ by choosing a uniform random deviate over the 1σ range quoted by Gebhardt et al. (2000) (we obtain indistinguishable results when a Gaussian random deviate is used). Interestingly, we see no evidence of a trend in $\langle M_{\rm BH}/M_{\rm gal}\rangle$ with halo mass.

However, this result is not strongly conclusive, because it is not known whether the relationship between $M_{\rm BH}$ and $\sigma_{\rm e}$ depends on halo mass. However, these results are suggestive that there may be too much black hole growth via the 'radio mode' in the models, perhaps indicating that other heating processes *not associated with black hole growth* may also be important in quenching cooling flows.

We caution, as well, that although it is tempting to try to interpret the 'fine features' in these diagrams, the assignment of halo masses in the current SDSS group catalogues is not very precise (see the Appendix), and therefore only broad statistical trends should be taken seriously. It is possible that in the future, if more precise estimates of individual halo masses become available for large samples, for example from gravitational lensing or X-rays, we may be able to investigate these predicted trends in more detail.

5 DISCUSSION AND CONCLUSIONS

In this paper, we set out to investigate the significance of internal galaxy properties versus environment in shaping the star formation history of galaxies, and to attempt to understand some of the physical processes that might be at work. We made use of the observational group catalogue constructed from SDSS DR4 and the NYU-VAGC (Y07). The group catalogue provides an estimate of the halo mass for each group, which can be directly compared with semi-analytic models. These halo mass estimates should provide a more unbiased probe of global environment than measures based on local galaxy density (e.g. distance to the nth nearest neighbour).[2]

We have also used a subsample of SDSS with GALEX coverage to estimate SFRs (S07), which should be a more direct probe of the physics of star formation quenching than optical colours. Besides, we make use of semi-analytic models from several independent groups (S08, dL06 and MORGANA), and containing different sets of recipes representing physical processes.

We first investigated the global distribution of colour versus magnitude and SSFR versus stellar mass in the five models we considered, compared with the empirical data. Although the different models showed some differences in the details of their predictions for these quantities, the models with some kind of quenching (either due to AGN feedback or according to a critical halo mass) have similar qualitative features and on the whole are a reasonable match to the empirical data – not surprisingly, as these observational quantities have been a target for theoretical models for some time. We therefore found that it was sensible to identify active or quenched galaxies according to either a CM criterion (the usual 'green valley') or a similar SSFR–$M_{\rm gal}$ criterion.

Next, we investigated the stellar mass dependence of the quenched fraction based on optical colours ($f_{\rm red}$) or on SSFR determined from SDSS + GALEX photometry ($f_{\rm passive}$). Here, we largely confirmed and reproduced results shown previously by other authors (though our results in terms of SSFR from GALEX are new), namely that the fraction of red/passive galaxies increases with stellar mass for both central and satellite galaxies, and that the models with AGN feedback or halo mass based quenching reproduce this trend reasonably well for central galaxies, but fail badly for satellites. All of the models produce too high a fraction of red satellites and too flat a dependence of quenching on stellar mass, which we term the *satellite overquenching problem*.

We then investigated the joint dependence of quenched fraction ($f_{\rm red}$ and $f_{\rm passive}$) on galaxy mass and halo mass. First, we investigated $f_{\rm red}$ and $f_{\rm passive}$ as a function of halo mass, in different stellar mass bins. A difficulty with this approach was that, especially for central galaxies, there is quite a limited range of stellar masses in haloes of a given mass. Our analysis showed that, for central galaxies in the observational group catalogues, the fraction of quenched galaxies shows a strong dependence on halo mass at fixed stellar mass, but also shows a strong dependence on stellar mass at fixed halo mass. We were not able to determine which quantity is the primary driver of quenching. The S08 fiducial and dL06 models reproduced these trends fairly well. For observed satellite galaxies, there was a much stronger dependence on stellar mass visible in the $f_{\rm red}$ diagram (based on optical colours) and a weaker trend in the $f_{\rm passive}$ diagram (based on UV-derived SSFR). Once again, all models failed to reproduce the satellite properties, and even showed an inverted trend in $f_{\rm passive}$ with respect to the empirical data.

We also found it interesting to look at the pattern of $f_{\rm red}$ and $f_{\rm passive}$ in terms of the two-dimensional ($M_{\rm halo}$–$M_{\rm gal}$) plane. This analysis revealed that the contours of $f_{\rm red}$ and $f_{\rm passive}$ for central galaxies can be interpreted as either a horizontal run or a vertical run, again due to the degeneracy between halo mass and central galaxy mass. The models showed quite a different pattern in this space, and tended to show stronger vertical boundaries, indicating a stronger dependence on halo mass. For both the empirical data and the models, these diagrams demonstrate the complexity of the interplay between halo mass and stellar mass, and are a promising tool for posing stringent tests on physical recipes in galaxy formation models. However, we caution that the estimates of halo mass in the SDSS group catalogues are statistical in nature, and this may introduce distortions into these distributions (see Appendix).

We attempted to probe the physical origin of these results by exploring additional correlations, such as the fraction of morphologically early-type (spheroid-dominated) galaxies in the observed sample, $f_{\rm early}$. We found a strikingly similar pattern for $f_{\rm early}$ in the ($M_{\rm halo}$, $M_{\rm gal}$) plane as we did for $f_{\rm red}$ and $f_{\rm passive}$, suggesting that these quantities are tightly linked in some way. One natural possibility is that the bulge mass is correlated with the mass of a supermassive black hole, and that the black hole mass, in turn, controls the quenching of star formation. Intriguingly, we found that in the models with black hole regulated AGN heating (S08 fiducial and dL06), the galaxies that were most likely to be blue, actively star forming and disc dominated were expected to be those with the smallest black hole for their mass. In addition, we saw a trend with halo mass, in the sense that central galaxies in larger mass haloes are able to grow black holes more efficiently (the ratio of black hole mass to stellar mass is larger). These trends were much

[2] But note that some groups have started measuring galaxy number densities using search ellipsoids large enough to be representative of massive cluster haloes (e.g. Schawinski et al. 2007a; Yoon et al. 2008).

weaker or absent in models in which the black hole is not involved in regulating cooling (such as the 'halo-quenching' model). We do not have direct estimates of black hole masses for large samples of galaxies, but we used the measured SDSS velocity dispersion σ_e and the observed M_{BH}–σ_e relation to obtain estimates of a black hole mass proxy, M_σ. We do not see a strong trend in M_σ/M_{gal} for the SDSS group catalogue, indicating that either this method for estimating the empirical black hole masses is too crude or the dependence of black hole mass on halo mass in the models is too strong.

Although the model predictions for the distribution of f_{red} and $f_{passive}$ in the (M_{halo}, M_{gal}) plane do not match the observational results in detail, we conclude that the observational data are consistent with the basic qualitative picture presented by the models in which cooling is regulated by AGN feedback at least for central galaxies. In these models, the suppression of cooling and the quenching of star formation depend on two factors: the presence of a quasi-hydrostatic hot halo (strongly correlated with halo mass) and the mass of the supermassive black hole (strongly correlated with galaxy mass). This picture is also strongly supported by the recent work of Pasquali et al. (2008), which directly explored the dependence of 'radio-mode' and 'bright-mode' AGN activity on halo mass and stellar mass in these same SDSS group catalogues. The empirical data do not seem to support models in which the process that suppresses cooling is solely a function of halo mass (e.g. Dekel & Birnboim 2008; Khochfar & Ostriker 2008), although it will be important to explore the explicit predictions of alternate heating mechanisms (such as heating by clumps or infalling satellites) in detail.

The MORGANA model suffers from the largest disagreement with the observations. The treatment of the triggering of 'radio-mode' accretion in MORGANA is significantly different than in the other two models, requiring that star formation is inevitably associated with the triggering of radio-mode accretion. Although the radio-mode feedback mechanism adopted in MORGANA is largely able to solve the 'overcooling problem' in terms of reproducing the galaxy stellar mass or luminosity function, this star formation makes many massive galaxies too blue. Our analysis places tight constraints on the links between star formation and AGN activity at late times, and highlights our current lack of understanding of the details of the processes that regulate both kinds of activity.

For satellite galaxies, the empirical diagrams suggested that quenching depends on *both* stellar mass and halo mass, such that the 'critical stellar mass' that divides active from passive (blue from red) galaxies decreases with increasing halo mass. None of the models was successful in predicting this trend. Including tidal destruction of satellites, as was done in the S08 models, improves the agreement with the data because satellites that have been orbiting for a long time within the host halo (which tend to be red and passive) are destroyed. However, it seems that tidal destruction cannot provide a full solution to the problem.

The problems with overquenching of satellites in semi-analytic models have been demonstrated before (e.g. Weinmann et al. 2006b) and are likely due to the assumption applied in nearly all SAMs that the hot gas halo, which is the source of new cooling gas, is stripped off instantly when a galaxy becomes a satellite in a larger halo (sometimes called 'strangulation'). Therefore, satellites fairly quickly consume their remaining cold gas reservoirs and become red and passive (e.g. Crowl & Kenney 2006). However, recent hydrodynamic simulations have found that the hot gas haloes of satellites are not stripped instantly (Kawata & Mulchaey 2008; McCarthy et al. 2008). Recently, several authors (Font et al. 2008; Kang & van den Bosch 2008) have proposed improved recipes for the treatment of cooling on to satellites, which produce better results for the predictions of satellite colours. Clearly, our analysis should be repeated with one of these improved treatments implemented in our models. However, it is probably also important to properly treat the effects of ram pressure stripping on both the satellites' hot halo and the cold gas in the galaxy (Quilis et al. 2000; Okamoto & Nagashima 2003; Lanzoni et al. 2005). This will clearly be an important area for improvements to the modelling and further investigations.

ACKNOWLEDGMENTS

The empirical data derived from the Sloan Digital Sky Survey and the Galaxy Evolution Explorer observations played a critical role in this project. We warmly thank G. de Lucia and G. Lemson for help with the Millennium catalogues and data base server, and Sadegh Khochfar and Marc Sarzi for numerous insightful discussions. We are also grateful to the referee for several important clarifications. SKY acknowledges support from the Basic Research Program of the Korea Science and Engineering Foundation (R01-2006-000-10716-0). TK is grateful for the hospitality of the Max-Planck-Institut für Astronomie in Heidelberg during his visit. FF and PM thank Laura Silva for help in the use of GRASIL. Some of the calculations were carried out at the PIA cluster of the Max-Planck-Institut für Astronomie at the Rechenzentrum Garching.

REFERENCES

Abadi M. G., Moore B., Bower R. G., 1999, MNRAS, 308, 947
Adelman-McCarthy J. K. et al., 2006, ApJS, 162, 38
Baldry I. K. et al., 2004, ApJ, 600, 681
Baldry I. K., Balogh M. L., Bower R. G., Glazebrook K., Nichol R. C., Bamford S. P., Budavari T., 2006, MNRAS, 373, 469
Balogh M. L., Morris S. M., 2000, MNRAS, 318, 703
Balogh M. L. et al., 2004, ApJ, 615, L101
Barnes J. E., 2002, MNRAS, 333, 481
Bell F. E., McIntosh D. H., Katz N., Weinberg M. D., 2003, ApJ, 149, 289
Bell F. E. et al., 2004, ApJ, 608, 752
Bekki K., Couch W. J., Shioya Y., 2002, ApJ, 577, 651
Benson A. J., Bower R. G., Frenk C. S., Baugh C. M., Cole S., 2003, ApJ, 599, 38
Best P. N. et al., 2005, MNRAS, 362, 25
Birnboim Y., Dekel A., 2003, MNRAS, 345, 349
Blanton M. R. et al., 2003, AJ, 125, 2348
Blanton M. R. et al., 2005a, AJ, 129, 2562
Blanton M. R. et al., 2005b, ApJ, 629, 143
Blanton M. R., Roweis S., 2007, AJ, 133, 734
Bower R. G. et al., 2006, MNRAS, 370, 645
Boylan-Kolchin M., Ma C. -P., Quataert E., 2008, MNRAS, 383, 93
Bruzual G., Charlot S., 2003, MNRAS, 344, 1000
Cattaneo A., Dekel A., Devriendt J., Guiderdoni B., Blaizot J., 2006, MNRAS, 370, 1651
Chandrasekhar S., 1943, ApJ, 97, 255
Christlein D., Zabludoff A., 2005, ApJ, 621, 201
Chung A., van Gorkom J. H., Kenney J. D. P., Vollmer B., 2007, ApJ, 659, L115
Coil A. L. et al., 2008, ApJ, 672, 153
Cooper M. C. et al., 2006, MNRAS, 370, 198
Cole S., Lacey C. G., Baugh C. M., Frenk C. S., 2000, MNRAS, 319, 168
Cox T. J., Primack J., Jonsson P., Somerville R. S., 2004, ApJ, 607, L87
Croton D. et al., 2006, MNRAS, 365, 11
Crowl H. H., Kenney J. D. P., 2006, ApJ, 649, L75
Davis M., Geller M. J., 1976, ApJ, 208, 13
Davis M., Efstathiou G., Frenk C. S., White S. D. M., 1985, ApJ, 292, 371
De Lucia G., Blaizot J., 2007, MNRAS, 375, 2

De Lucia G., Springel V., White S. D. M., Croton D., Kauffmann G., 2006, MNRAS, 366, 499 (dL06)
Dekel A., Silk J., 1986, ApJ, 303, 39
Dekel A., Birnboim Y., 2006, MNRAS, 368, 2
Dekel A., Birnboim Y., 2008, MNRAS, 383, 119
Di Matteo T., Springel V., Hernquist L., 2005, Nat, 433, 604
Dressler A., 1980, ApJ, 236, 351
Font A. S. et al., 2008, MNRAS, 389, 1619
Fontanot F., Monaco P., Cristiani S., Tozzi P., 2006, MNRAS, 373, 1173
Fontanot F., Monaco P., Silva L., Grazian A., 2007, MNRAS, 382, 903
Fontanot F., De Lucia G., Monaco P., Somerville R. S., Santini P., 2009, preprint (arXiv:0901.1130)
Gebhardt K. et al., 2000, ApJ, 539, L13
Granato G. L., De Zotti G., Silva L., Bressan A., Danese L., 2004, ApJ, 600, 580
Gomez P. L. et al., 2003, ApJ, 584, 210
Gunn J. E., Gott J. R., 1972, ApJ, 176, 1
Hashimoto Y., Oemler A., Lin H., Tucker D. L., 1998, ApJ, 499, 589
Hatton S., Devriendt J. E. G., Ninin S., Bouchet F. R., Guiderdoni B., Vibert D., 2003, MNRAS, 343, 75
Hopkins P. F., Hernquist L., Cox T. J., Robertson B., Krause E., 2007, ApJ, 669, 45
Kang X., van den Bosch F. C., 2008, ApJ, 676, L101
Kang X., Jing Y. P., Mo H. J., Borner G., 2005, ApJ, 631, 21
Kauffmann G., White S. D. M., Guiderdoni B., 1993, MNRAS, 264, 201
Kauffmann G., Colberg J. M., Diaferio A., White S. D. M., 1999, MNRAS, 303, 188
Kauffmann G. et al., 2003, MNRAS, 341, 54
Kauffmann G., White S. D. M., Heckman T. M., Ménard B., Brinchmann J., Charlot S., Tremonti C., Brinkmann J., 2004, MNRAS, 353, 713
Kaviraj S. et al., 2007, ApJS, 173, 619
Kawata D., Mulchaey J. S., 2008, ApJ, 672, L103
Kennicutt R. C., 1989, ApJ, 344, 685
Kennicutt R. C., 1998, ApJ, 498, 181
Kereš D., Katz N., Weinberg D. H., Davé R., 2005, MNRAS, 363, 2
Khochfar S., Burkert A., 2003, ApJ, 597, L117
Khochfar S., Burkert A., 2005, MNRAS, 359, 1379
Khochfar S., Ostriker J., 2008, MNRAS, 680, 54
Lanzoni B., Guiderdoni B., Mamon G. A., Devriendt J., Hatton S., 2005, MNRAS, 361, 369
Larson R. B., 1974, MNRAS, 169, 229
Larson R. B., Tinsely B. M., Caldwell C. N., 1980, ApJ, 237, 692
Lewis I. et al., 2002, MNRAS, 334, 673
McCarthy I. G., Frenk C. S., Font A. S., Lacey C. G., Bower R. G., Mitchell N. L., Balogh M. L., Theuns T., 2008, MNRAS, 383, 593
McNamara B. R., Nulsen P. E. J., 2007, ARA&A, 45, 117
Martin C. L., Kennicutt R. C., 2001, ApJ, 555, 301
Martin D. C. et al., 2005, ApJ, 619, 1
Mo H. J., Mao S., White S. D. M., 1998, MNRAS, 295, 319
Monaco P., 2004, MNRAS, 352, 181
Monaco P., Fontanot F., 2005, MNRAS, 359, 283
Monaco P., Theuns T., Taffoni G., 2002, MNRAS, 331, 587
Monaco P., Fontanot F., Taffoni G., 2007, MNRAS, 375, 1189
Moore B., Lake G., Katz N., 1998, ApJ, 495, 139
Murray N., Quataert E., Thompson T. A., 2005, ApJ, 618, 569
Navarro J. F., Frenk C. S., White S. D. M., 1997, ApJ, 490, 493 (NFW)
Nulsen P. E. J., Fabian A. C., 2000, MNRAS, 311, 346
Okamoto T., Nagashima M., 2003, ApJ, 587, 500
Quilis V., Moore B., Bower R., 2000, Sci, 288, 1617
Pasquali A., van den Bosch F. C., Mo H. J., Yang X., Somerville R. S., 2008, preprint (arXiv:0807.4178)
Poggianti B. M. et al., 2006, ApJ, 642, 188
Roberts M. S., Haynes M. P., 1994, ARA&A, 32, 115
Salim S. et al., 2007, ApJS, 173, 267 (S07)
Schawinski K. et al., 2006, Nat, 442, 888
Schawinski K. et al., 2007a, ApJS, 173, 512
Schawinski K. et al., 2007b, MNRAS, 382, 1415
Schmidt M., 1968, ApJ, 151, 393
Shimasaku K. et al., 2001, AJ, 122, 1238
Silk J., Rees M. J., 1998, A&A, 331, L1
Silva L., Granato G. L., Bressan A., Danese L., 1998, ApJ, 509, 103
Somerville R. S., Kolatt T. S., 1999, MNRAS, 305, 1
Somerville R. S., Primack J. R., 1999, MNRAS, 310, 1087
Somerville R. S., Primack J. R., Faber S. M., 2001, MNRAS, 320, 504
Somerville et al., 2008a, ApJ, 672, 776
Somerville R. S., Hopkins P. F., Cox T. J., Robertson B. E., Hernquist L., 2008b, MNRAS, 391, 480 (S08)
Strateva I. et al., 2001, AJ, 122, 1861
Springel V., White S. D. M., Tormen G., Kauffmann G., 2001, MNRAS, 328, 726
Springel V. et al., 2005, Nat, 435, 629
Springel V., Di Matteo T., Hernquist L., 2005, MNRAS, 361, 776
Taffoni G., Mayer L., Colpi M., Governato F., 2003, MNRAS, 341, 434
Tanaka M., Goto T., Okamura S., Shimasaku K., Brinkmann J., 2004, ApJ, 128, 2677
Taylor J. E., Babul A., 2004, MNRAS, 348, 811
Toomre A., Toomre J., 1972, ApJ, 178, 623
Umemura M., 2001, ApJ, 560, L29
van den Bosch F. C., Aquino D., Yang X., Mo H. J., Pasquali A., McIntosh D. H., Weinmann S. M., Kang X., 2008a, MNRAS, 387, 79
van den Bosch F. C., Pasquali A., Yang X., Mo H. J., Weinmann S., McIntosh D. H., Aquino D., 2008b, preprint (arXiv:0805.0002)
Viola M., Monaco P., Borgani S., Murante G., Tornatore L., 2008, MNRAS, 383, 777
Warren M. S., Abazajian K., Holz D. E., Teodoro L., 2006, ApJ, 646, 881
Weinmann S. M., van den Bosch F. C., Yang X., Mo H. J., 2006a, MNRAS, 366, 2 (W06a)
Weinmann S. M. et al., 2006b, MNRAS, 372, 1161
Weinmann S. M., Kauffmann G., van den Bosch F. C., Pasquali A., McIntosh D. H., Mo H. J., Yang X., Guo Y., 2008, preprint (arXiv:0809.2283)
White S. D. M., Frenk C. S., 1991, ApJ, 379, 52
Yang X., Mo H. J., van den Bosch F. C., Jing Y. P., 2005, MNRAS, 356, 1293
Yang X., Mo H. J., van den Bosch F. C., Pasquali A., Li C., Barden M., 2007, ApJ, 671, 153 (Y07)
Yi S. K. et al., 2005, ApJ, 619, L111
Yoon J. H., Schawinski K., Sheen Y.-K., Ree C. H., Yi S. K., 2008, ApJS, 176, 414
Zentner A. R., Bullock J. S., 2003, ApJ, 598, 49

APPENDIX A: THE EFFECT OF DUST, SELECTION CRITERIA AND GROUP CATALOGUE HALO MASS ESTIMATES

All of our models include a treatment of dust extinction, which affects both the colours and magnitudes of the model galaxies. In addition, as mentioned in Section 4, for our main analysis we have applied selection criteria to the models to mimic those that we believe to be present in the SDSS group catalogue. We include only galaxies with apparent r-band magnitude brighter than 17.77 mag, and we also excluded haloes which do not contain any galaxy member brighter than ${}^{0.1}M_r \leq -19.5 + 5\log h$. In this Appendix, we provide the results for the two-dimensional distributions of $f_{\rm red}$ and $f_{\rm passive}$ for the theoretical models without dust extinction and without selection criteria applied. In addition, we test for possible biases that may arise from the approach used to assign halo masses to the groups in the SDSS group catalogues by applying this method to the model mock catalogues.

In Fig. A1, we show $f_{\rm red}$ and $f_{\rm passive}$ without any dust corrections applied to the models. Since we do not have magnitude information without dust corrections for the dL06 models, only the S08 fiducial and MORGANA models are shown. Interestingly, the results now look much more similar to the results seen before for $f_{\rm passive}$. In particular,

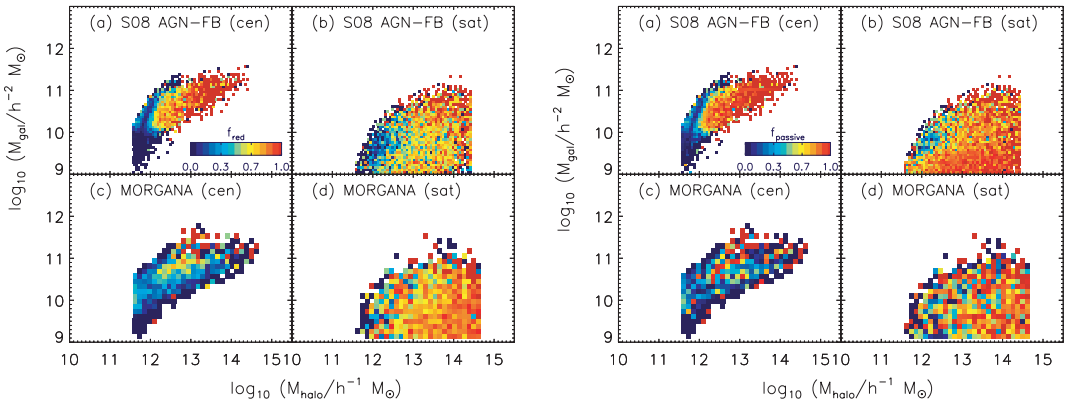

Figure A1. The fraction of 'red' ($f_{\rm red}$; left-hand panels) and 'passive' galaxies ($f_{\rm passive}$; right-hand panels) in models without dust corrections. The colour scale is as in Fig. 6. We present the results for central galaxies (left-hand panel) and satellite (right-hand panel) galaxies separately. We see that the details of the $f_{\rm red}$ distribution are quite sensitive to the dust correction, whereas $f_{\rm passive}$ is not notably affected by the dust correction. We also note that the dust-free $f_{\rm red}$ results appear more similar to the $f_{\rm passive}$ results, which presumably probe the physical properties of galaxies more directly.

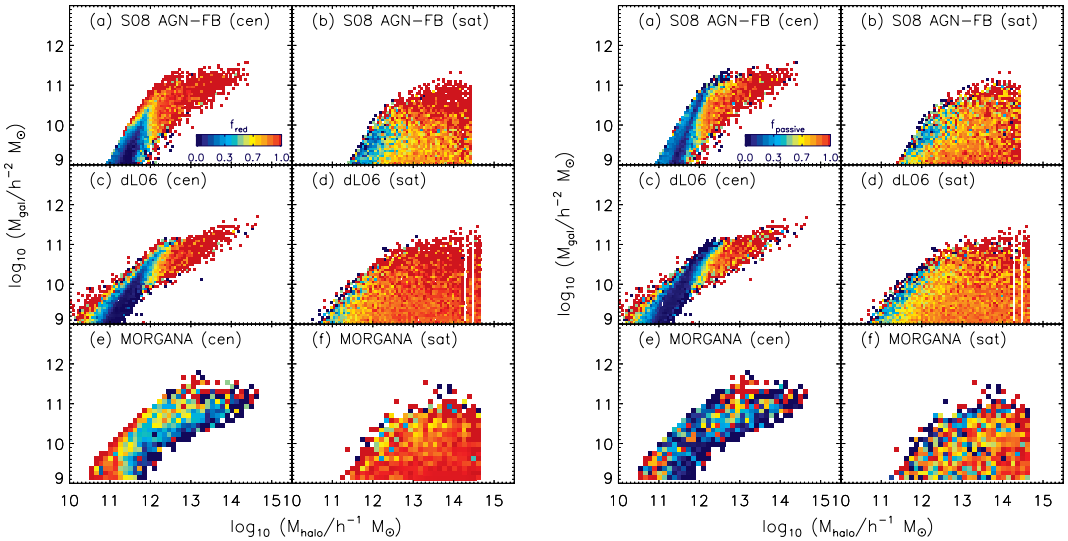

Figure A2. The fraction of 'red' galaxies ($f_{\rm red}$) (left panels) and of 'passive' galaxies ($f_{\rm passive}$) (right panels) without selection criteria. The colour scale is as in Fig. 6. We present the results for central galaxies (left) and satellite (right) galaxies separately. It can be inferred that our main results do not depend on our selection criteria.

the blue ridge which was visible in the $f_{\rm passive}$ diagrams corresponded to a *red* ridge in the $f_{\rm red}$ diagram (Fig. 6). The blue ridge is now visible in $f_{\rm red}$ as well, indicating that these galaxies are actually actively star forming, and were predicted to be red only because of dust extinction. In the case of $f_{\rm passive}$, the dust correction only affects the galaxy selection and causes a negligible change in the diagrams. The treatment of dust extinction is one of the most uncertain aspects of the modelling, and this highlights the advantage of using intrinsic physical quantities extracted from the observations.

Fig. A2 shows the model predictions with no selection effects applied. Comparing this with Fig. 6, we see that the results appear unchanged above a halo mass $\log M_{\rm halo}\,h^{-1}\,{\rm M}_{\odot} \geq 11.6$ and a stellar mass $M_{\rm gal} \geq 10^9\,{\rm M}_{\odot}$. This is reassuring in the context of our present analysis. However, we can also see that there is interesting predicted behaviour at lower halo and galaxy masses than we can currently probe, and also interesting differences between the models at these masses. This suggests that it would be extremely useful to obtain similar data that are complete to fainter levels, so that we could probe lower mass galaxies and lower mass haloes.

Finally, we investigate the procedure used to assign halo masses to the groups that are identified in the SDSS group catalogue. For the results presented here, stellar masses for several models are obtained from Bell et al. (2003) like Y07, and halo masses are assigned based on the 'characteristic' stellar mass of the group, where the characteristic stellar mass is defined as the total stellar mass contributed by galaxies with ${}^{0.1}M_r \leq -19.5 + 5\log h$. Halo masses are then assigned by matching the rank-ordered list of group characteristic stellar masses with a rank-ordered list of DMH masses from a theoretical estimate of the DM halo mass function, assuming a monotonic mapping between the characteristic stellar mass and DM halo mass (see Section 2.1 and Y07). We apply this procedure to the haloes in the mock catalogue produced with the S08 fiducial semi-analytic model, and show the comparison between the true and estimated halo mass in Fig. A3. We see that although

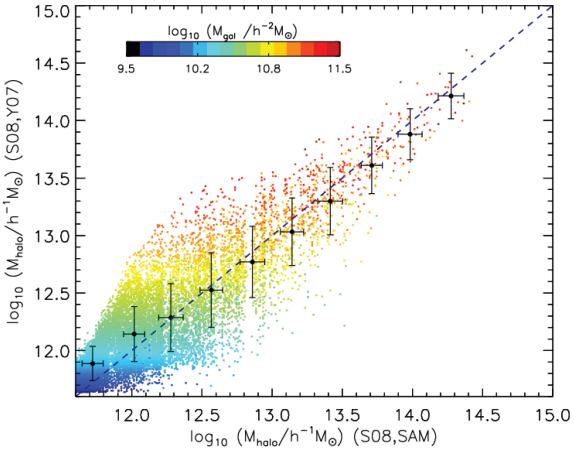

Figure A3. The true halo mass in the fiducial semi-analytic model of S08, compared with the halo mass estimate based on the total stellar mass in the halo, using a procedure similar to that of Y07 for the SDSS-based group catalogue. The colour scale indicates the stellar mass of the central galaxy in each halo, as shown by the key on the figure. Although the mean halo mass is reproduced fairly well, there is quite a large scatter in the true halo mass at a given estimated halo mass.

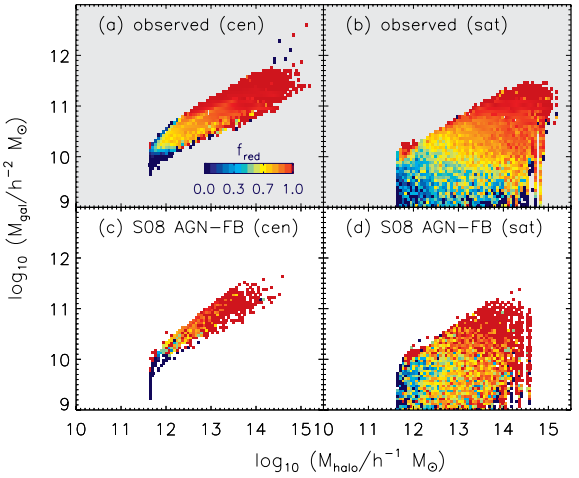

Figure A4. The fraction of 'red' galaxies ($f_{\rm red}$) as a function of halo mass and stellar mass, where halo masses have been assigned in the semi-analytic models using an approach similar to that used in the SDSS group catalogues. The colour scale is as in Fig. 6. We present the results for central galaxies (left-hand panel) and satellite (right-hand panel) galaxies separately. We see that the procedure used to assign halo masses in the SDSS group catalogues reduces the scatter in $M_{\rm gal}$ at a fixed halo mass, and washes out many of the detailed features of the two-dimensional distribution that are visible in the raw model predictions.

the mean halo mass is estimated fairly accurately, there is a large scatter in true halo mass at a given value of the estimated halo mass.

In Fig. A4, we show again the distribution of $f_{\rm red}$ with halo mass and stellar mass, now using the Y07-like halo mass estimates for the semi-analytic models instead of the true halo masses. We see that the procedure artificially reduces the scatter in $M_{\rm gal}$ at fixed halo mass. This can be attributed to two effects. First, the halo mass estimates in the Y07 group catalogue are based on the total stellar mass in the halo, which strongly correlates with the stellar mass of the central galaxy. In addition, the Y07 group catalogue includes corrections for various incompleteness effects in the SDSS (the factor C in equations 3–4 in Y07), which creates scatter that is not visible in the mock catalogues. It should also be noted that the halo mass estimating algorithm of Y07 washes out many of the detailed features that are visible in the model predictions. Hence, we should not make too much of the detailed features in the empirical $M_{\rm gal}$–$M_{\rm halo}$ diagrams but should focus on the mean trends instead.

This paper has been typeset from a TEX/LATEX file prepared by the author.